

Binding of Au³⁺ Ions by Polyadenine DNA

by

Yichen Zhao

A thesis

presented to the University of Waterloo

in fulfillment of the

thesis requirement for the degree of

Master of Science

in

Chemistry (Nanotechnology)

Waterloo, Ontario, Canada, 2020

© Yichen Zhao 2020

Author's Declaration

I hereby declare that I am the sole author of this thesis. This is a true copy of the thesis, including any required final revisions, as accepted by my examiners.

I understand that my thesis may be made electronically available to the public.

Abstract

Interactions between DNA and metal ions are important for many applications such as metal sensing, therapeutics and nanotechnology. Many studies have already been published on these topics. DNA can bind metal ions via its phosphate backbone and the nucleobases. The phosphate backbone likes to bind hard metal ions, whereas the bases tend to coordinate with softer metal ions. Gold in particular is one metal that has many interactions with DNA. Gold nanoparticles are very stable and DNA-functionalized nanoparticles have been used for biosensing, drug delivery and the design of smart materials. However, many of these studies have been carried out on gold surfaces where gold has an oxidation state of zero. The study of the interactions between gold ions (Au^{3+}) and DNA has been limited. Au^{3+} is a highly soft metal ion and it may have strong interactions with DNA bases. The goal of this thesis is to study the interactions between gold ions and DNA.

Fluorescein (FAM) labelled 15-mer homopolymer DNA (FAM- A_{15} , C_{15} , G_{15} , and T_{15}) were first incubated with a source of Au^{3+} ions (HAuCl_4). The reaction products were characterized by denaturing gel electrophoresis and kinetic studies were done using fluorescence quenching assays. In the electrophoresis studies, little to no products were observed with T_{15} and C_{15} DNA. A smearing of the gel electrophoresis bands along with some fluorescence quenching was observed with both A_{15} and G_{15} DNA suggesting stable complex formation that survived the denaturing gel electrophoresis conditions. A_{15} DNA showed complete reaction, while G_{15} showed around 80% reaction yield after 1 hour.

Since poly-A DNA showed the highest activity for binding to Au^{3+} , studies of the formation of the polyadenine – Au^{3+} complex were then conducted as a function of pH and salt. Complex formation was favored at a lower pH (pH 4) and would not form under higher pH (pH

8) conditions. Salt was found to be required for Au^{3+} to react with DNA. Four different salts (NaF, NaCl, NaBr, and NaI) were tested to see the effects on binding kinetics. The addition of NaF and NaI did not allow the formation of the Au^{3+} -poly-A complex, but NaCl and NaBr allowed the formation of this complex. Therefore, a moderate affinity ligand such as Cl^- and Br^- favored the reaction. A random 24mer DNA was then compared to A_{15} for binding to Au^{3+} and other metal ions. Both DNA only showed evidence of complex formation with Au^{3+} and not with other metals including Hg^{2+} and Pb^{2+} .

Fluorescence quenching assays of A_{15} and Au^{3+} were done as a function of concentration of different salts. First order kinetic rate constants were found to be 0.60 mins^{-1} , 0.91 mins^{-1} , 1.5 mins^{-1} , and 1.9 mins^{-1} for buffers with no salt, 100 mM NaBr, 100 mM NaCl, and 10 mM NaBr respectively. This reaction was also found to be reversible as the fluorescence could be recovered using potassium cyanide (KCN) or glutathione (GSH). When added post complex formation, KCN could recover almost all the fluorescence while GSH could recover around 60%.

The effects of Au^{3+} ions on the catalytic activity of the 17E zinc dependent DNAzyme were also studied using gel electrophoresis. Under normal conditions, 17E cleaves an RNA substrate with a cleavage percent of 71%, however with concentrations of 25 mM Au^{3+} and above, the cleavage of the substrate was completely inhibited. The Au^{3+} was found to be binding to the DNAzyme-substrate duplex in a similar fashion to A_{15} .

Acknowledgements

I would like to thank Dr. Juewen Liu for his continued guidance and mentorship on this project as well as the opportunity to pursue my graduate studies in his laboratory. I also extend my thanks to my committee members, Dr. Anna Klinkova and Dr. Vivek Maheshwari for being on my committee and providing helpful feedback on my work. Finally, I would like to thank all the members of the Liu group for their continued help and support.

Table of Contents

Author's Declaration.....	ii
Abstract.....	iii
Acknowledgements.....	v
List of Figures.....	viii
List of Tables.....	xi
List of Abbreviations.....	xii
Chapter 1 – Introduction.....	1
1.1. Structure of DNA.....	1
1.2 Metal/DNA Interactions.....	4
1.3 Gold.....	9
1.3.1. DNA adsorption on AuNPs.....	9
1.3.2. DNA Interaction with Gold Ions.....	16
1.4 Au ³⁺ Detection.....	19
1.5 Thesis Objective.....	23
Chapter 2 - Binding of Au ³⁺ by DNA oligonucleotides.....	24
2.1 Introduction.....	24
2.2 Experimental Methods.....	25
2.2.1 Chemicals Used.....	25
2.2.2 Gel Electrophoresis.....	25
2.2.3 Fluorescence Spectroscopy.....	28
2.2.4 Buffers.....	28
2.3 Results and Discussion.....	29
2.3.1 A ₁₅ , C ₁₅ , G ₁₅ , T ₁₅ DNA binding to Au ³⁺	29
2.3.2 Binding of Au ³⁺ by A ₁₅ as a function of Salt.....	33
2.3.3 Stable Binding of Au ³⁺	37
2.3.4 Fluorescence Studies.....	39
2.3.5 Fluorescence Recovery.....	41
2.4 Conclusions.....	42
Chapter 3 - Effect of Au ³⁺ on DNAzyme activity.....	44
3.1 Introduction.....	44
3.2 Experimental.....	47

3.2.1 DNAzyme preparation	47
3.2.2 Activity assay	48
3.3 Results and Discussion	48
3.3.1 DNAzyme activity in the presence of Zn ²⁺	48
3.3.2 Effect of soft metal ions on the activity	50
3.3.3 Discussion	51
3.4 Conclusions.....	52
Chapter 4 - Conclusions and Future Work.....	53
4.1 Conclusions.....	53
4.2 Future Work.....	54
Chapter 5 - Lab Safety	55
References.....	56

List of Figures

Figure 1.1 The structure of nucleobases, nucleosides (nucleobase + deoxyribose), and nucleotides (nucleobase + deoxyribose + phosphate groups).	2
Figure 1.2 Watson-Crick (circled) and Hoogsteen base pairs.	2
Figure 1.3 A) Outer sphere coordination to hydrated metal complexes B) monodentate inner sphere coordination C) bidentate inner sphere coordination.	4
Figure 1.4 Multiple metal binding sites on thymine (top) and cytosine (bottom).	5
Figure 1.5 logK of binding sites on nucleoside monophosphates measured using potentiometric pH titration.	7
Figure 1.6 Differences between metal-modified and metal-mediated coordination.	8
Figure 1.7 Watson-Crick base pairs, pyrimidine mis-pairs, and metal mediated base pairs.	9
Figure 1.8 Binding trend of DNA bases to AuNP.	10
Figure 1.9 Tandem and terminal S modifications.	12
Figure 1.10. The preparation of AuNP-DNA conjugates by freezing.	14
Figure 1.11 Poly(A) duplex binding to AuNPs.	14
Figure 1.12 A) The coordination of adenine and gold B) the bottom up self-assembly of spherical colloid.	17
Figure 1.13 Gold and adenine fluorescent complex.	17
Figure 1.14 A) Binding of metals and adenine containing substances B) Complex aggregates and the sensing of single stranded DNA.	18

Figure 1.15 A) Schematic of the poly-A electrochemical gold sensor B) alternating current voltammetry graphs of different length sensors with the addition of gold ions.....	20
Figure 1.16 A) Fluorescence of sensor when tested with different metals B) structure of phosphine sensor C) proposed reaction scheme for gold sensing.....	21
Figure 1.17 Au ³⁺ inhibits the aggregation of fluorosurfactant capped AuNPs causing a color change.....	22
Figure 2.1 Polymerization of acrylamide, the reaction is initiated by persulphate radicals and catalyzed by tetramethylethylenediamine (TEMED).....	25
Figure 2.2 Urea denaturing the secondary structure of double stranded DNA.....	26
Figure 2.3 Binding of 90 μM gold ions with 1 μM FAM-A ₁₅ DNA, FAM-G ₁₅ , FAM-T ₁₅ , and FAM-C ₁₅ DNA	28
Figure 2.4 Effect of different salts at different concentrations.....	33
Figure 2.5 A) Relative fluorescence intensity post-electrophoresis of different buffer salts B) comparison of NaCl and NaBr buffer salts.....	34
Figure 2.6 A possible scheme for Au ³⁺ binding with adenine in A ₁₅	34
Figure 2.7 Binding of gold, lead, and mercury ions.....	36
Figure 2.8 Effects of gold on complementary DNA.....	37
Figure 2.9 Kinetic effects of using NaCl and NaBr as buffer salts in pH 4 acetate buffer.....	38
Figure 2.10 Fluorescence recovery using potassium cyanide (KCN), glutathione (GSH), and free adenosine.....	40

Figure 3.1 Examples of DNAzymes a) “10-23” DNAzyme with RNA cleaving activity b) “8-17” DNAzyme with RNA cleaving activity.....44

Figure 3.2 Cleavage action of 17E DNAzyme on a substrate catalyzed by metal ions.....44

Figure 3.3 Possible mechanism of DNAzyme cleavage. **A)** negative charge stabilization of oxygen atom, **B)** activation of the nucleophilic hydroxyl by deprotonation or coordination, **C)** stabilization of the negative charge built-up on the oxygen of the leaving group, **D)** general base catalysis.....45

Figure 3.4 The cleavage action of 17E with regards to Zn^{2+} concentration.....48

Figure 3.5 **A)** The effects of Au^{3+} , Hg^{2+} , and Cu^{2+} ions on the action of 17E **B)** A graph quantifying the drop in cleavage.....49

List of Tables

Table 1. pK _a values of the nucleic acids and backbone phosphate.....	3
Table 2. Sequences of DNA used in experiments	24
Table 3. Formation constants with Au ³⁺	35
Table 4. First order rate constants.....	39
Table 5. Sequences of 17E and PO substrate.....	46

List of Abbreviations

A	Adenine
APS	Ammonium Persulfate
AuNP	Gold Nanoparticles
C	Cytosine
DNA	Deoxyribonucleic acid
EDTA	Ethylenediaminetetraacetic acid
FAM	6-Carboxyfluorescein
FSN	Fluorosurfactant Capped Nanoparticles
G	Guanine
M	Molarity (mol/liter)
MES	2-(<i>N</i> -morpholino) ethanesulfonic acid
RNA	Ribonucleic acid
TEMED	N,N,N',N'-Tetramethylethylenediamine
T	Thymine
UV	Ultraviolet Light

Chapter 1 – Introduction

DNA (deoxyribonucleic acid) is our genetic material. As a biopolymer, DNA can have many different applications in biotechnology and nanotechnology. For example, its different interactions with many metals makes DNA a prime candidate for biosensing and drug development.¹ DNA has been used and studied as a sensor to detect metal ions since the early 2000s.² Its many bases can coordinate with metals to form useful structures and complexes. One of the most studied applications is cisplatin binding to DNA for cancer therapy.³ In addition, DNA can also be combined with nanoparticles to form better sensors. By functionalizing the surface of metallic (such as silver or gold) nanoparticles with DNA, new sensors can be developed to detect a wide range of analytes.⁴

1.1. Structure of DNA

The structure of DNA molecules consists of a nucleobase, a pentose sugar, and a phosphate group. There are 4 different nucleobases possible for DNA (adenine (A), guanine(G), cytosine (C), thymine (T)) as shown in Figure 1.1.⁵ These 4 bases can then be separated again into purines and pyrimidines. The pyrimidines have a single carbon ring with nitrogen at the 1 and 3 positions. The pyrimidine bases are cytosine and thymine in DNA. Purines are a pyrimidine ring fused together with an imidazole. They contain 2 carbon rings with 4 nitrogen atoms. The purine bases are adenine and guanine.

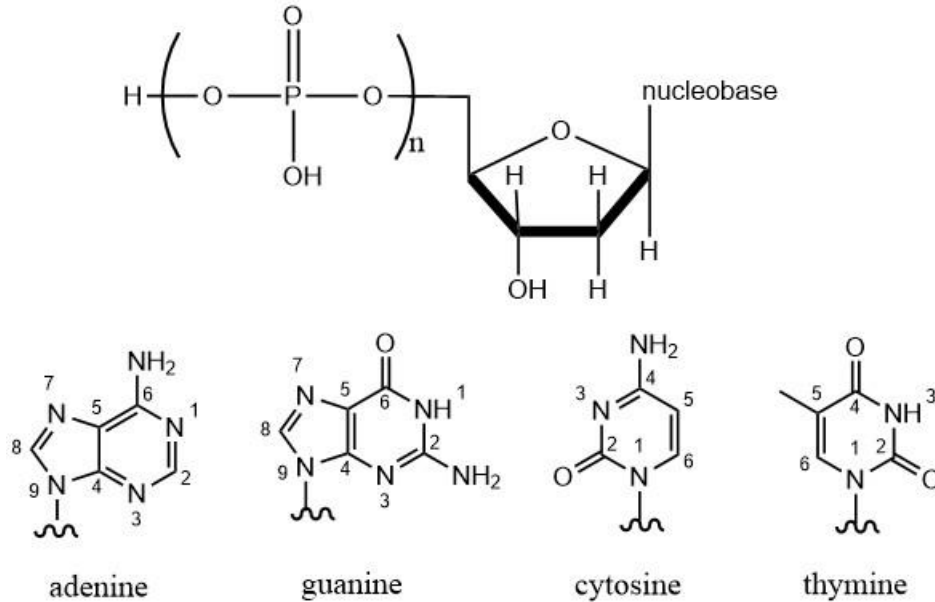


Figure 1.1 The structure of nucleobases, nucleosides (nucleobase + deoxyribose), and nucleotides (nucleobase + deoxyribose + phosphate groups).

In a usual DNA duplex, these bases are paired up (A and T, G and C) and use hydrogen bonding to stabilize the double helical structure of DNA. There are two common types of pairing that occur, Watson-Crick pairs and Hoogsteen pairs. For the A-T Watson-Crick pairing, hydrogen bonds are formed between the N1 and C6 amino groups on the adenine to the N3 and C4 oxygen on the thymine. The Hoogsteen A-T pair uses the N7 and C6 amino from the adenine bound to the N3 and C4 oxygen of thymine. The Watson-Crick pairing of G-C uses the C6 oxygen, N1, and C2 amino groups from the guanine bound to the C4 amino, N3, and C2 oxygen of cytosine. The Hoogsten G-C pair uses N7 and the C6 oxygen on guanine bound to N3 and the C4 amino on cytosine. Figure 1.2 shows the differences between these two pairings.⁶

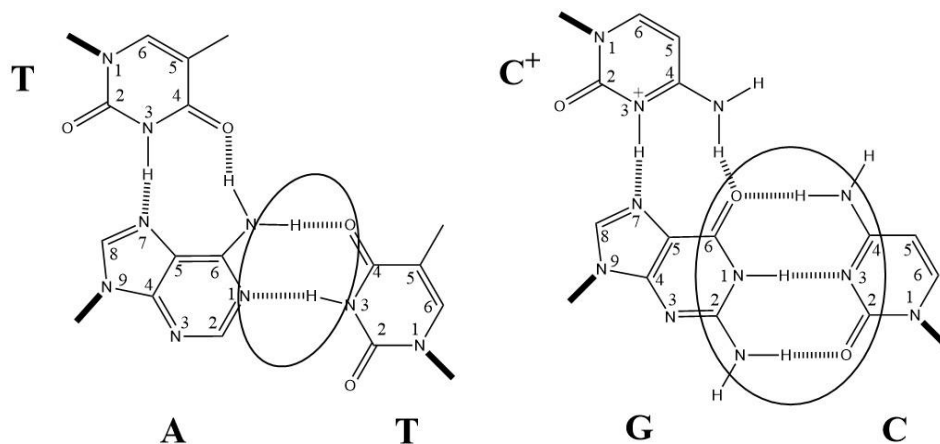


Figure 1.2 Watson-Crick (circled) and Hoogsteen base pairs.

Each DNA base as well as the phosphate backbone has acidic hydrogens and can exist in its protonated or deprotonated state according to their site specific pK_a values (Table 1). At physiological pH, the backbone phosphate is deprotonated, and each phosphate carries one negative charge. On the other hand, all four nucleobases are charge neutral at physiological pH. Therefore, overall, the DNA is highly negatively charged. At low pH, such as pH 3, adenine and cytosine are protonated. This can affect both the stability and structure of DNA, as well as its metal binding properties.

Table 1. pK_a values of the nucleic acids and backbone phosphate.

DNA Component	pK_a value
Backbone Phosphate	~2
Adenine	N7 (3.5)
Cytosine	N3 (4.2)
Guanine	N7 (2.1), N1 (9.2)
Thymine	N3 (9.9)

1.2 Metal/DNA Interactions

Since DNA is polyanionic, electrostatic attraction can occur with metal ions. Metal ions interact with either the phosphate backbone, which stabilizes the DNA duplex, or DNA bases, which may destabilize the DNA duplex. Coordination with metal ions can be described as either “inner sphere” coordination or “outer sphere” coordination. By coordinating with the inner sphere, ligands are interacting directly with the metal ion itself (Figure 1.3B). Outer sphere coordination occurs through an intermediary ligand. An example of outer sphere coordination is the coordination hydrated metal ions; the ligand is first binds to the water that is then directly bound to the metal (Figure 1.3A). Denticity is another factor to consider in the coordination of metal ions. Denticity refers to the number of groups that a single ligand can bind to the central metal in a coordination complex (Figure 1.3C).

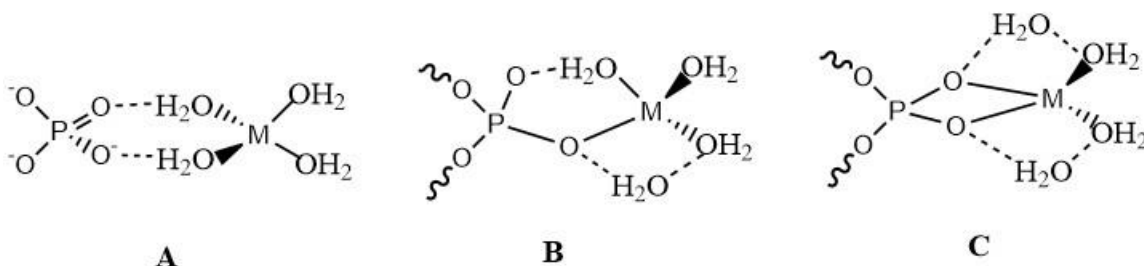


Figure 1.3 A) Outer sphere coordination to hydrated metal complexes B) monodentate inner sphere coordination C) bidentate inner sphere coordination.

Since the phosphate backbone is negatively charged, metal cations can be used to stabilize this charge. Cations such as the group I alkali metals (Li^+ , Na^+ , K^+ , Cs^+) are found to preferentially bind the phosphate backbone. Group I metals showed no change in binding when the base composition of the DNA was altered, showing that these metals are binding to the

phosphates and not the nucleic acids themselves. Of these metals, Li^+ was found to have the highest outer sphere affinity through its role as a counterion while the other metals (Na^+ , K^+) preferred inner sphere coordination.⁷ Group II metals such as Mg^{2+} and Ca^{2+} were also found to have a higher affinity for the DNA backbone than the bases.^{8,9} However, transition metals were found to interact and form complexes with the DNA bases. The phosphate backbone tends to bind harder metals since they stabilize the DNA while the bases tend to bind softer metals.⁸

The DNA bases and metal ions can interact through either non-covalent interactions or coordinative bonding. Non-covalent interactions include electrostatic attraction, outer sphere binding through hydrogen bonds, intercalation, or binding through van der Waals forces. This type of binding usually refers to a coordinatively saturated species which is irrespective of the metal ions or ligands.¹⁰ Coordinative binding refers to the inner sphere binding of metals directly with donor sites on the DNA bases. These coordinative bonds tend to be reversible so the metal can usually be displaced by a strong nucleophile.¹¹ The affinity for different ions can vary with its coordination with each nucleobase. There are multiple sites that can bind metallic ions. Cytosine can have binding sites at N3, N4, O2, and C5. Thymine binding can occur at N3 (as seen in Figure 1.4)¹².

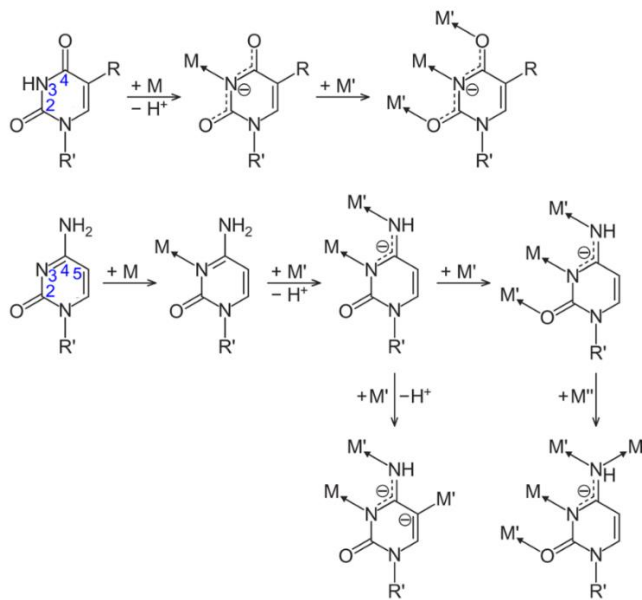


Figure 1.4 Multiple metal binding sites on thymine (top) and cytosine (bottom). Adapted with permission from reference 13. Copyright 2016 American Chemical Society.

Adenine can coordinate with metals using N6 from the amino, N1, N3, N7 and N9. Binding sites in guanine are N1, N7 and O6.¹² However, the purine N3 site is generally sterically hindered by the sugar and has weak binding, but changing the relative orientation of the base and sugar can make this site available.¹⁴ It has been shown that in duplex DNA, adenine has favored N7 over other sites but in isolated adenine bases, both N1 and N7 are good binding sites. N7 is the favored site for guanine binding but can cross over to N1 in acidic pH.¹⁵ The binding sites are also pH dependent. Some sites such as the N1 in guanosine and N3 in thymidine are only available upon deprotonation. The exocyclic amino groups in adenine (N6) and cytosine (N4) normally would not bind metal ions, however these sites may be able to bind in special cases, such as in a rare tautomer form. These rare tautomer forms can also be induced by metal entities. For example, the N6 of adenine can bind to Hg^{2+} when N1 is protonated (imino tautomer of adenine)^{16,17} and the N4 of cytosine can bind Pt ions when N3 is protonated (imino-oxo

tautomer).^{16,18} All of these binding sites can bind alone or in conjunction with each other (i.e. chelation) to form different complexes with a wide variety of metals. Both the phosphate and the DNA base can be involved in coordinating a single metal, such as the binding of Cu^{2+} ions to the N7 site of guanine and the phosphate group in guanosine monophosphate (GMP).¹⁹

Different binding sites also have different affinities for different metals. The affinity for a metal to bind to certain sites can be quantified with stability constants (K). This constant can be thought of as the equilibrium constant between the metal ion and the metal complex formed with the nucleoside. Some log stability constants for common metals and nucleoside monophosphates can be found in Figure 1.5. These constants have already been adjusted with a factor accounting for the phosphate group.⁸

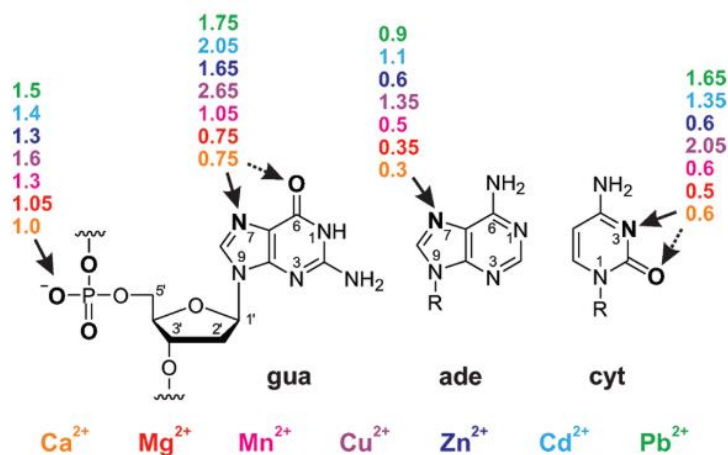


Figure 1.5 logK of binding sites on nucleoside monophosphates measured using potentiometric pH titrations. Adapted with permission from reference 8. Copyright 2010 American Chemical Society.

These stability constants show that when coordinating with metal ions, the phosphate is more involved in coordinating hard metals (such as group I and II) while the binding sites on the individual bases have a higher affinity for softer metals (transition metals).

Metals can also modify the base pairing of nucleobases. By replacing weakly acidic nucleobase protons by metal ions of preferably linear, trans square planar, or trans octahedral coordination geometries, the hydrogen bond formation between their constituents can be modified (Figure 1.6).¹³

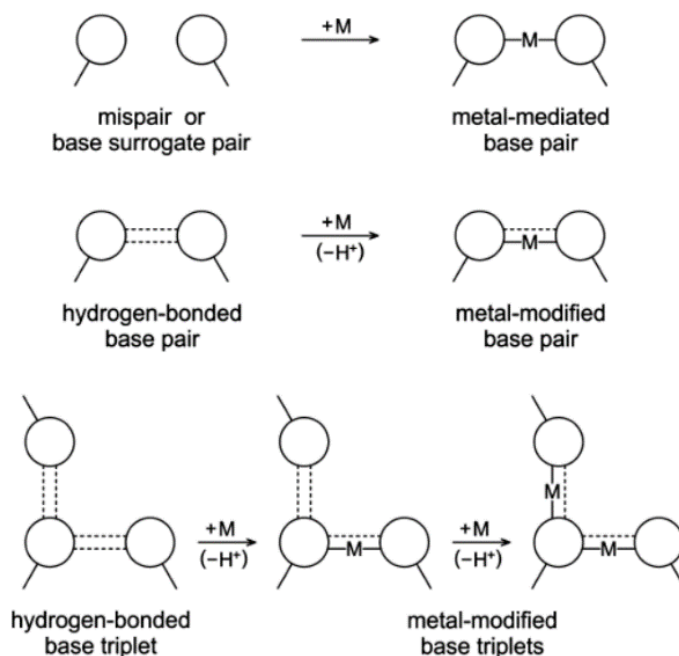


Figure 1.6 Differences between metal-modified and metal-mediated coordination. Adapted with permission from reference 13. Copyright 2016 American Chemical Society.

Some well known metal mediated base pairs in the DNA duplex include the T-Hg-T and C-Ag-C metallo-base pairs.²⁰ Mercury and silver ions are known to bind to nucleobases preferentially.⁵ A complex containing a 2:1 ratio of 1-methylthymine to Hg(II) ions has been reported and a ratio of 1:1 Ag ion to C-C pair was confirmed.²⁰ Figure 1.7 shows the proposed binding schemes of T-Hg-T and C-Ag-C.

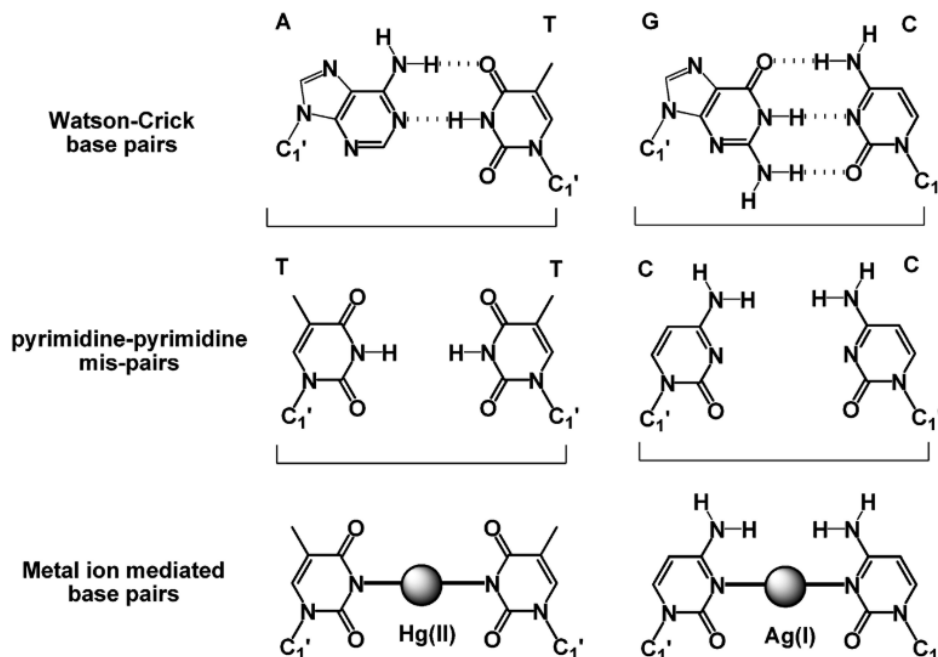


Figure 1.7 Watson-Crick base pairs, pyrimidine mis-pairs, and metal mediated base pairs. Figure adapted from reference 20. Republished with permission of Royal Society of Chemistry, from Binding of metal ions by pyrimidine base pairs in DNA duplexes, Ono, A., Torigoe, H., Tanaka, Y. & Okamoto, I., 40, 2011; permission conveyed through Copyright Clearance Center, Inc. "

1.3 Gold

1.3.1. DNA adsorption on AuNPs

Gold is a metal that comes in many forms and has many applications. One of the most well studied forms of gold is gold nanoparticles (AuNPs). AuNPs have excellent plasmonic properties, such as a high extinction coefficients,²¹ that allow them to have unique optical properties (light scattering, color changes, etc.) at very low concentrations (nanomolar to picomolar).²² They are also very good at quenching fluorescence (~99% quenched)²³ and have a high surface energy and can adsorb strongly to thiols, halides, and organic molecules such as nucleotides. Since traditional clean gold surfaces are hydrophilic, these surfaces can become easily contaminated when exposed to air leading to a large contact angle.²⁴ AuNPs are formed in

solution and can be kept free from contaminants resulting in more consistent surface properties that last for a longer time. By keeping the gold particles in solution, there is less surface area coming into direct contact with air, retaining more of its surface properties. The most common way that AuNPs are prepared for use with DNA is by the reduction of HAuCl_4 by citrate resulting in citrate stabilized AuNPs.²⁵ However, one of the challenges that AuNPs face is their colloidal stability. Factors such as salt concentration (i.e. can cause aggregation²⁶) and buffers (i.e. HEPES buffer can alter surface morphology²⁷) can change the colloidal properties of AuNPs.

As mentioned before, gold nanoparticles can adsorb DNA, making them an excellent vehicle for many applications. However, DNA is negatively charged due to the phosphate backbone since all of the nucleobases are in a neutral state (see Table 1). Therefore, without the addition of other charge stabilizers, there is little to no adsorption of DNA onto the citrate stabilized AuNPs due to long range electrostatic repulsions. In order to get higher adsorption, it was found that salt could be added to enhance activity. However, at high concentrations of salt, aggregation of the AuNPs was observed.²⁸

Another way the DNA could adsorb onto gold surfaces is through binding of the nucleic acids to the gold surface. The affinity of the nucleic acids to gold surfaces has been reported as adenine > cytosine > guanine > thymine (Figure 1.8).²⁹ The affinities of guanine and cytosine can vary depending on different measurements.

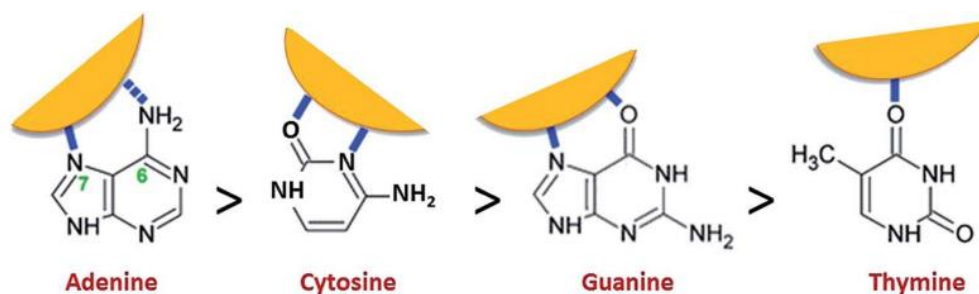


Figure 1.8 Binding trend of DNA bases to AuNPs. The solid lines represent the main interaction while the dotted line shows a weaker contribution. Figure adapted from reference 30. Republished with permission of Royal Society of Chemistry, DNA–bare gold affinity interactions: mechanism and applications in biosensing, Shiddiky, M. J. A., Koo, K. M., Trau, M., Carrascosa, L. G. & Sina, A. A. I, **7**, 2015; permission conveyed through Copyright Clearance Center, Inc. "

In adenine, the exocyclic amino group at the N6 position and a N7 ring nitrogen enables a high adsorption affinity. This strong adsorption is strong enough that even in the presence of complementary poly-T DNA, poly-A DNA still stably adsorbs to neutral gold surfaces.²⁹ The binding mechanism takes place through a direct interaction of the ring's nitrogen with gold as well as a partial contribution from the exocyclic amino group.³⁰ Guanine compounds were suggested to bind through the C6 ketone together with the N1 nitrogen or through the C6 ketone group and the N7 nitrogen.^{31,32} Cytosine and its derivatives were suggested to bind through the N3 nitrogen as well as the keto oxygen.³¹ Thymine has the weakest binding through only the C4 keto oxygen.³¹

Another suggested trend for the binding affinities of nucleobases is the order: guanine > adenine > cytosine > thymine.³³ These trend differences for each base can be explained through their individual adsorption processes. While adenine showed the highest affinity through chemisorption, thermal desorption studies showed that guanine had higher temperature values.³⁴ This could be due to fact that guanine have more interactions between each other leading to a

more stable gold-guanine aggregate as opposed to the adsorption of individual guanines onto gold surfaces.^{30,34}

Since the DNA and the citrate capped AuNPs are both negatively charged, other factors must be considered in order to achieve adsorption such as thiolation, charge screening by adjusting the salt concentration, pH, and other environmental factors.

Thiols have a very high (higher than the nucleic acids) affinity for gold surfaces. Therefore, many AuNP- DNA conjugates are made using thiolated DNA. There are two types of thiol modifications, a terminal modification and a tandem modification (PS as opposed to PO). The terminal modification is the addition of a thiol group usually in the form of 5'-SH-(CH₂) group to a 5' terminal oxygen while a PS modification is the replacement of a nonbridging phosphate oxygen with S (Figure 1.9). While both showed much higher adsorption of DNA when compared to non-thiolated DNA, the PS modification had higher affinity than the terminal modification.³⁵⁻³⁷ Debates around the nature and exact mechanisms of the SH – Au surface bond (predominantly chemisorbed or physisorbed) are still being studied.³⁸ However, the knowledge of this strong binding has been widely used in nanobiotechnology for its colloidal stabilization of AuNPs while allowing the DNA to still be functional (one of the key challenges in creating AuNP- DNA bioconjugates).

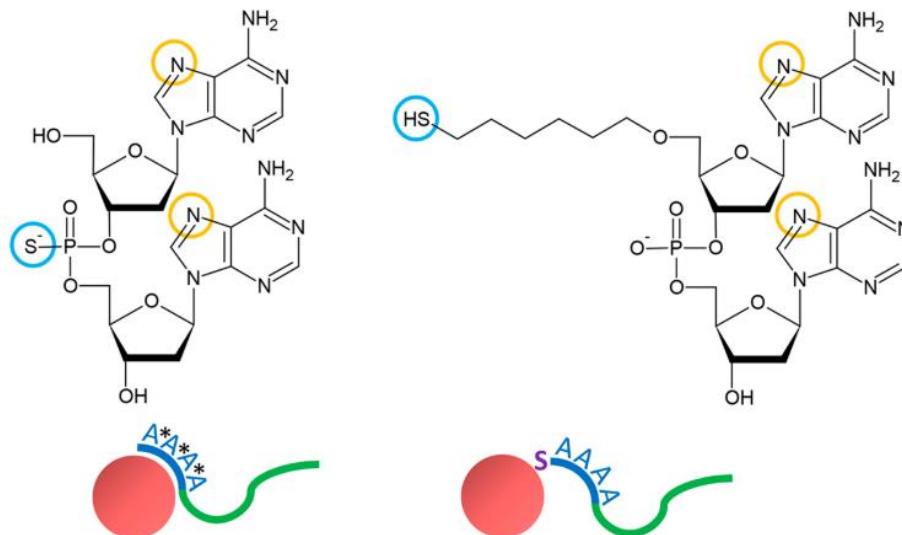


Figure 1.9 Tandem and terminal S modifications. Figure adapted with permission from reference 37. Copyright 2014 American Chemical Society.

As mentioned above salt is necessary to reduce long range charge repulsion but presents other problems by inducing the aggregation of AuNPs at relatively low concentrations (millimolar range to see aggregation).²⁸ The size of the cation also plays a role in both the adsorption kinetics as well as the final DNA density. One study showed that in group 1A and 2A metals, larger cations (such as Cs^+) allowed better initial adsorption kinetics but smaller cations (such as Li^+) yielded a higher density of thiolated DNA after an incubation period.³⁹ Anions also play a role in the adsorption of DNA to AuNPs. Halides can compete with DNA to bind to the gold surface with larger halides having greater affinity and the ability to displace other bindings with a trend of $\text{F}^- < \text{T}^- \approx \text{Cl}^- < \text{C}^- < \text{G}^- \approx \text{Br}^- < \text{A}^- < \text{I}^-$.^{40,41}

Since the addition of large quantities of salt can cause unwanted aggregation of AuNPs, the salt aging method⁴² was proposed as a way of using salt to create AuNP-DNA conjugates without aggregation. The slow addition of salt (0.05 M – 0.1 M increments, up to ~0.7 M) over a long period of time in the presence of a PEG spacer allowed significantly more DNA loading on

to the AuNPs. The addition of surfactants can also help reduce the aging time by reducing the sticking of the AuNPs to each other and walls of the vial.⁴²

The pH of the environment also affects the binding affinity and stability of DNA to AuNPs. At neutral pH, the DNA bases are all charge neutral but start to protonate/deprotonate at three pH units away from neutral. The duplex starts to break down when the pH is below 4.5 or above 9.⁴³ Lowering the pH below 3 allows the DNA backbone to be partially stabilized by the protonated adenine and cytosine and has also been shown to accelerate DNA adsorption⁴⁴ due to the formation of secondary structures of adenine (poly-A parallel duplex).^{45,46}

It was reported that AuNP-DNA conjugates could also be formed by simply freezing and thawing the necessary reagents. It was hypothesized that the formation of ice crystals pushed the DNA, AuNPs, and salt into “micropockets” which concentrated them and enhanced the reaction rate (Figure 1.10).⁴⁷ An excess of DNA needs to be added to maintain colloidal stability. The freezing of the AuNP-DNA mixture also caused the DNA to stretch and align itself in an upright conformation.^{48,49}

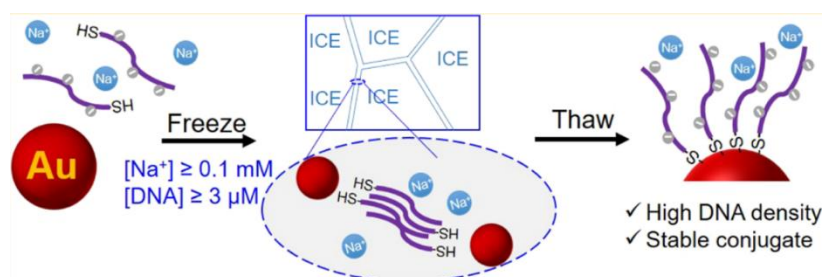


Figure 1.10. The preparation of AuNP-DNA conjugates by freezing. Figure adapted with permission from reference 49. Copyright 2019 American Chemical Society.

The affinity of the bases for gold surfaces can also be used to form these bioconjugates. A non-thiolated diblock DNA with a poly-A anchor was reported. Due to the high affinity that

adenine has for gold surfaces, the poly-A portion of the DNA serves as an anchor and a spacer, allowing the rest of the strand to still be functional and able to hybridize.⁵⁰ Adenine has also been used at lower pH levels through the formation of the poly-A duplex. By attaching a poly-A segment to random DNA, it readily exposes the thiol group to react directly with the gold surface and reduces the chance of nonspecific DNA base binding (Figure 1.11). The poly-A motif was found to be superior to other base motifs such as the i-motif (poly-C) and poly-G in terms of stability.⁴⁵

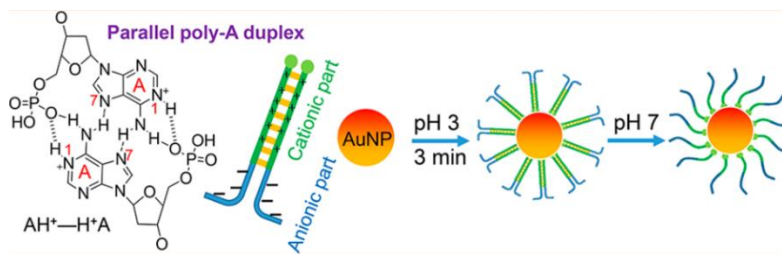


Figure 1.11 Poly(A) duplex binding to AuNPs. Adapted with permission from reference 45.

Copyright 2016 American Chemical Society.

Aside from binding simple oligonucleotides, more complex structures such as tetrahedron DNA have also been attached to gold surfaces serving as a spacer to retain the functions of biomolecules attached to it.⁵¹

Once these conjugates are synthesized, they can have a wide variety of applications in biosensing. They can be used as colorimetric sensors through the controlled aggregation of AuNP-DNA conjugates. These have very good detection limits.^{52,53} Due to the excellent fluorescence quenching abilities of AuNPs, sensors based around fluorescence quenching have also been developed. For example, the monitoring of DNA cleavage by nucleases⁵⁴ and the concept of nano-flares; detecting a fluorescent signal when a fluorophore labelled DNA detaches from the AuNP on the presence of other ligands.⁵⁵

1.3.2. DNA Interaction with Gold Ions

The interactions between gold ions and DNA have also been reported, though not to the extent that functionalized AuNPs have. Some forces involved in the interaction between gold and DNA include electrostatic interactions, hydrophobic forces, as well as specific binding between gold and the DNA bases.³⁰ The DNA bases have already been shown to interact with different heavy metals to coordinate around and form complexes. Au³⁺ has been found to be predominantly base binding instead of phosphate binding.⁵⁶

It has been reported in RNA duplexes, that Au³⁺ ions can perturb the binding of accessible G-C Watson-Crick base pairs by binding to the N3 and O2 sites in cytosine and the N2 and deprotonated N1 sites of guanine.⁵⁷ Although this binding did perturb the base pair it did not fully disrupt it. Also, due to the binding involving a deprotonated N1 site on guanine, this interaction may not occur at lower pH levels.

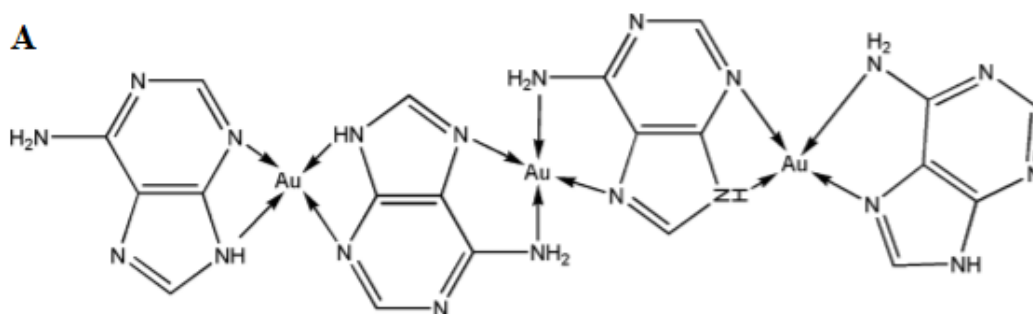
Oxidative halogenation at the C5 positions of uracil and cytosine along with the H₂O addition to the C5-C6 double bond and the oxidative dimerization of uracil ligands have both been observed due to the addition of [AuCl₄]⁻.⁵⁸

Thymine has generally been agreed upon to have the lowest affinity for gold. However, there have still been devices and methods involving thymine and gold for the sensing of heavy metals. One group developed a sensor for mercury ions based on the coordination of the thymine-mercury-thymine metal mediated base pair and gold nanoparticles.⁵⁹ The N3 site of thymine can bind metals such as Cu²⁺ and Pt²⁺ and could possibly bind Au³⁺ ions due to their similarity (Cu being in the same group and Pt being isoelectronic).⁵⁶

One study has found that there is some complexation of cytosine to Au^+ (gold (I)) ions at the N3 atom through nuclear magnetic resonance spectra analysis.⁶⁰ There is also evidence that cytosine can form a complex with $[\text{AuCl}_4]^-$ through binding at N3. X-ray crystallography was done on a complex of 1-methylcytosine and $[\text{AuCl}_4]^-$ and found three chlorine atoms and the N3 bound to gold forming a near square planar geometry (typical of Au^{3+} complexes). However, unless stabilized by the appropriate ligands, this complex would not last long in biological fluids due to the high oxidizing ability of gold.⁶¹ Organometallic complexes with Au^{3+} can also occur through C5 binding of cytosine and uracil along with C8 binding in purines.¹⁰

Guanine has also been found to bind Au^{3+} . The guanine quartet formed has been found to aid in the aggregation of gold nanoparticles.⁶² AuCl_3 has been shown to bind to the N7 position of guanine derivatives, but the purine skeleton will eventually be destroyed if kept in solution. It is suspected that this is due to oxidative degradation but is unconfirmed.⁶³

Adenine has the strongest affinity for gold ions. Adenine has many available sites (N1, N3, N7, N9, C6 amino)⁶⁴ but binding usually occurs at the N1 or N7 sites (Figure 1.12A).⁵⁶ Adenine has been known to coordinate with Au^{3+} ions to self-assemble and form colloidal spherical metal-adenine particles. The proposed mechanism for this self-assembly suggested that the π - π stacking as well as the interaction of the nitrogen atoms in adenine with gold ions were the dominant force (Figure 1.12B).⁶⁴



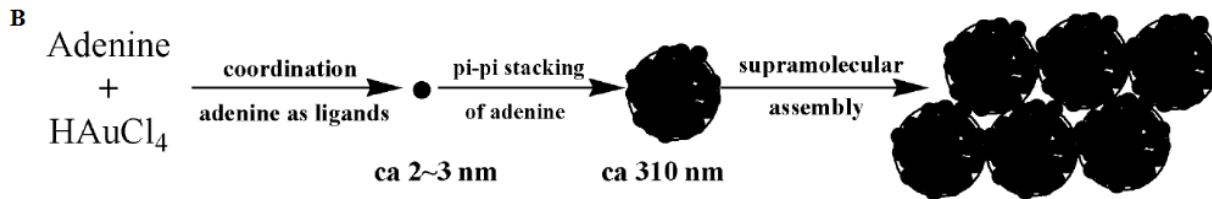


Figure 1.12 A) The coordination of adenine and gold B) the bottom up self-assembly of spherical colloids. Adapted with permission from reference 64. Copyright 2007 American Chemical Society.

Sensors have also been made from the interactions between adenine and gold. For example, a light activated gold and adenine (adenosine) complex was studied (Figure 1.13).

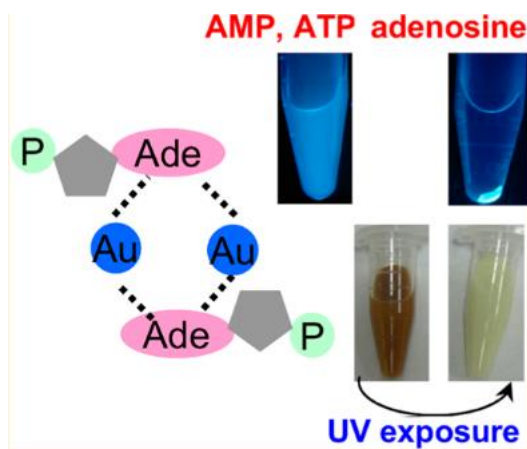


Figure 1.13 Gold and adenine fluorescent complex. Figure adapted from reference 65 with permission. Copyright 2013 American Chemical Society.

Knowing the different affinities of each nucleobase for gold, these properties can be used for biosensing and the development of biomaterials. For example, a new fluorescent material can be made from adenosine and gold ions.⁶⁵ Complexes formed from adenosine monophosphate and adenosine triphosphate have been identified as being able to produce fluorescence when exposed to light and heat.⁶⁵ This new material can provide many new applications in the analytical and biomedical fields.

Au³⁺ ions and adenine containing compounds have also found applications in the sensing of DNA strands.

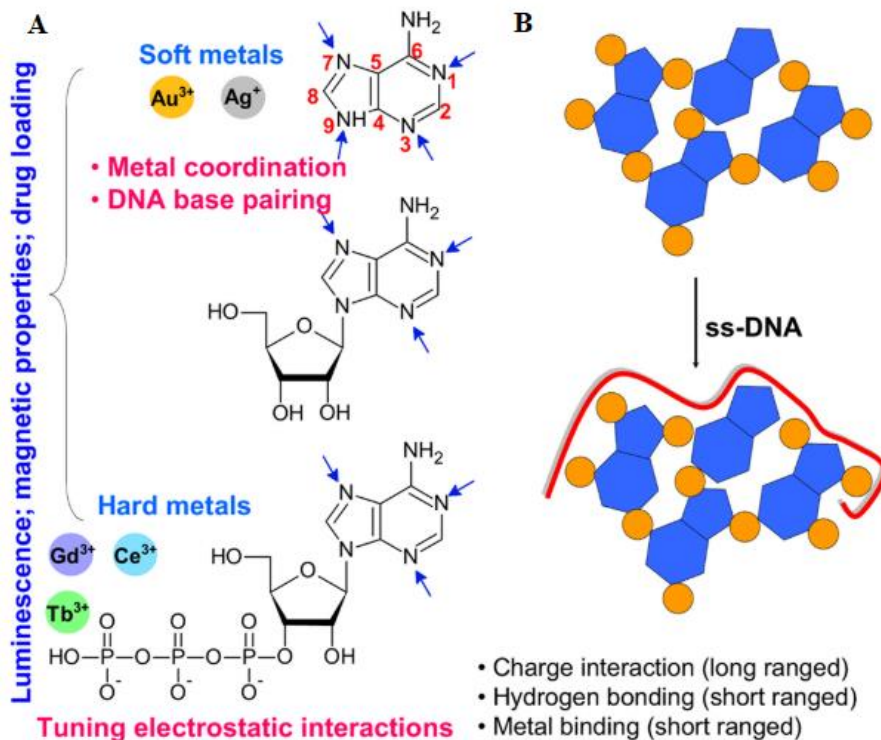


Figure 1.14 A) Binding of metals and adenine containing substances B) Complex aggregates and the sensing of single stranded DNA. Figure adapted with permission from reference 66. Copyright 2013 American Chemical Society.

Other metal ions were tested alongside gold to see the effect of different complexes. These gold-adenine complexes can detect single stranded DNA. Adsorption can be controlled by Watson-Crick base pairing and tuning surface charge while the adsorption strength can be controlled by the choice of metal ions (Figure 1.14B).⁶⁶

1.4 Au³⁺ Detection

Taking advantage of the strong affinity between adenine and gold, Wu and Lai employed oligoadenines as a recognition probe for the electrochemical detection of Au³⁺ ions. A6 (six

adenines) and A12 with methylene blue tags were used to sense the Au^{3+} ions by forming Au^{3+} and adenine complexes (Figure 1.15A).⁶⁷ These complexes would then change the current signal of the sensor (Figure 1.15B).⁶⁸ In the absence of Au^{3+} ions, the sensors are flexible allowing efficient electron transfer between the electrode and the tethered methylene blue. However, when Au^{3+} was added, the current decreased likely due to the formation of an Au^{3+} - adenine complex and increasing the rigidity of the sensor. This is then restricting access of the methylene blue to the electrode, leading to a measurable signal suppression. The limit of detection could be tuned simply by changing the length of the sensor (50 nM Au^{3+} for A6, 20 nM Au^{3+} for A12). The longer DNA had a lower signal recovery after regeneration possibly due to the incomplete removal of the target due to having more binding sites.

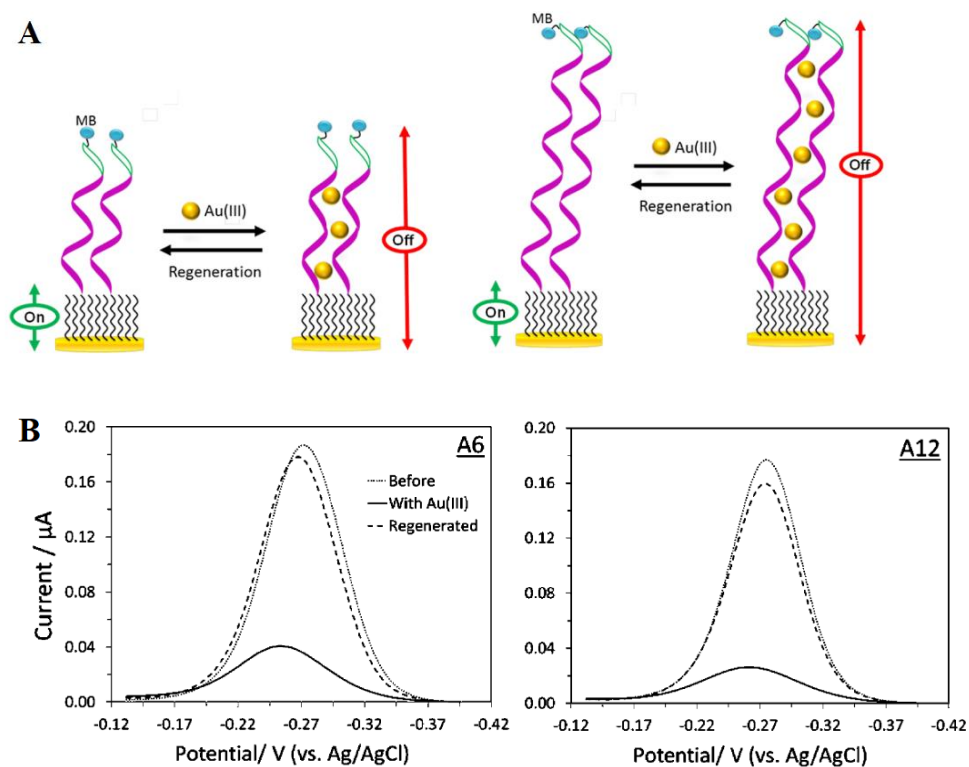


Figure 1.15 **A)** Schematic of the poly-A electrochemical gold sensor **B)** alternating current voltammetry graphs of different length sensors with the addition of gold ions. Figures adapted from reference 68 with permission. Copyright 2016 American Chemical Society.

A phosphine-labelled fluorescein derivative (Figure 1.16B) has also been discovered to be a good sensor for Au^{3+} ions (Figure 1.16A). This was due to a double “turn on” response in which the concurrent oxidation and coordination of the phosphine group produced the highly fluorescent phosphine oxide and phosphine gold chloride derivatives of the ligand.⁶⁹ The two turn on pathways are the oxidation of the phosphine group induced by the presence of Au^{3+} and the consequent reduction of Au^{3+} to Au^+ then coordinating with another phosphine group (Figure 1.16C).

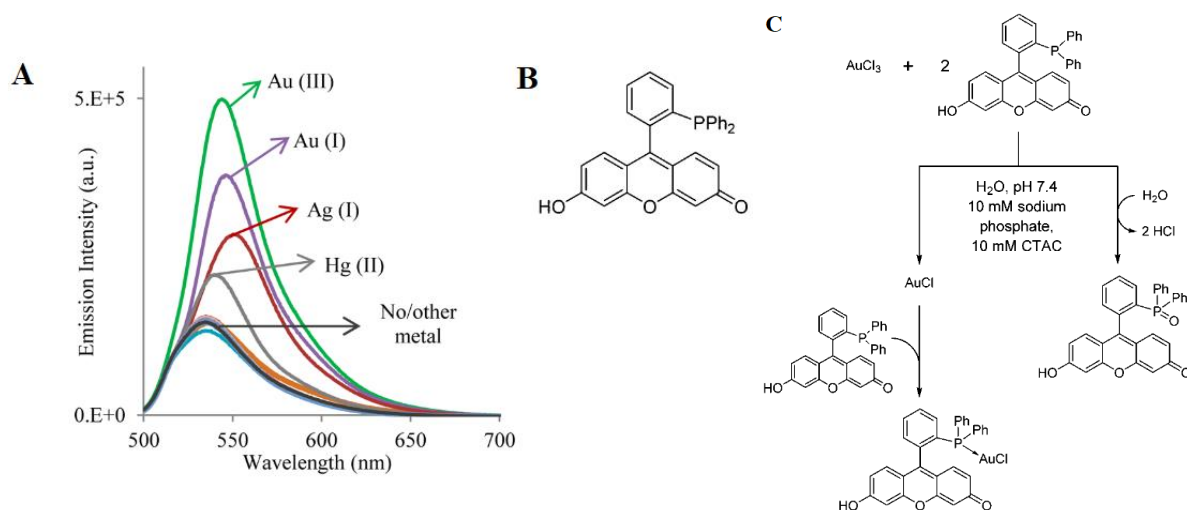


Figure 1.16 **A)** Fluorescence of sensor when tested with different metals **B)** structure of phosphine sensor **C)** proposed reaction scheme for gold sensing. Figure adapted from reference 69 with permission.

Copyright 2016 American Chemical Society.

Silver nanoparticles (AgNPs) have also been used for the detection of Au^{3+} ions. *N*-decanoyltromethamine was used as a stabilizing agent for the synthesis of AgNPs but was later

found to undergo decolorization in the presence of Au^{3+} ions. This sensing is based on a galvanic displacement reaction and has been applied to environmental water samples, being able to detect concentrations as low as $3.53 \mu\text{M Au}^{3+}$.⁷⁰

Functionalized AuNPs have also been used to detect Au^{3+} ions. A colorimetric sensor based on the aggregation of nonionic fluorosurfactant (FSN) capped AuNPs has been reported with a detection limit of around 50 nM Au^{3+} . Cysteine is known to trigger rapid aggregation of FSN-AuNPs in a high concentration of salt while its oxidized product (cystine) inhibits aggregation. Au^{3+} induces this oxidation and can therefore inhibit the aggregation of AuNPs, resulting in color changes (Figure 1.17).⁷¹

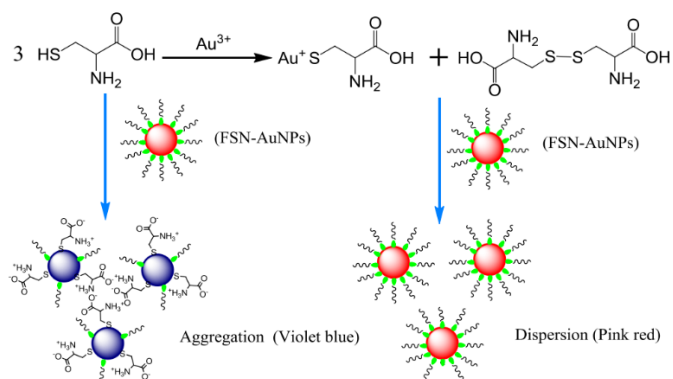


Figure 1.17 Au^{3+} inhibits the aggregation of fluorosurfactant capped AuNPs causing a color change.

Figure adapted from reference 71. Reprinted from *Biosensors and Bioelectronics*, 48, Bin Y., Xiao-Bing Z., Wei-Na L., Rong H, Weihong T, Guo-Li S, Ru-Qin Y, Fluorosurfactant-capped gold nanoparticles-based label-free colorimetric assay for Au^{3+} with tunable dynamic range via a redox strategy, 1-5, Copyright (2013), with permission from Elsevier.

Other fluorescent sensors for Au^{3+} include using a rhodamine derived alkyne probe that undergoes a ring opening and heterocycle formation resulting in a turn on fluorescence change⁷²

and using a latent fluorophore which undergoes a selective Au^{3+} - mediated hydroarylation reaction to turn on fluorescence.⁷³

1.5 Thesis Objective

Much of the research published focused on each nucleobase separately or in the form of their respective nucleotides and nucleosides. The study of gold in its +3 oxidation state and DNA is also limited. Due to this limited study, the effects and complications of gold ions on the functionality of DNA can be further explored. Given the strong binding between gold and DNA, we may discover distinct interactions different from other metal ions. The purpose of this research is to study these interactions between gold ions and homopolymer DNA. After this fundamental study, I was also interested in testing the possible effects gold ions may have on the function of DNA. For example, some DNA has catalytic activity (known as DNAzymes).⁷⁴ The effect of Au^{3+} on DNAzyme activity was also studied. By understanding the interactions between gold ions and homopolymer DNA, advances can be made in the field of DNAzymes, heavy metal detection, and biosensing.

Chapter 2 - Binding of Au³⁺ by DNA oligonucleotides

2.1 Introduction

The coordination of metal ions and DNA has been long studied. By looking at the interactions between metal ions and DNA, many conclusions have been drawn that led to the development of various devices for biosensing and a better understanding of how these interactions affect properties and structure of DNA. For example, the use of cisplatin in cancer therapy based on its ability to bind DNA.³ There are different affinities for different metals between the binding sites of the phosphate backbone and the different nucleobases. Metal ions have also been found to change the structure of duplex DNA by altering the base pairings such as the T-Hg-T and C-Ag-C metal mediated base pairs mentioned previously.

While there have been extensive studies on the reactions between gold surfaces and DNA, the interactions between the gold ions (Au³⁺) with DNA are more limited possibly due to the strong oxidation power of Au³⁺. There have been some studies reporting on some interactions between Au³⁺ and nucleotides and nucleosides^{11,61,63} as well as possible sensing methods.^{66,68,69,73} By studying the reactions between Au³⁺ and DNA, these interactions can have an impact on sensing, *in vitro* selection of DNA, and the effects on other functional DNA.

In this chapter, I aimed to study the effect of pH, salt concentration, and DNA sequence with respect to the reactions of Au³⁺ ions and single stranded DNA. The selectivity of Au³⁺ for A₁₅ DNA was also studied along with the reversibility of the formed complexes.

2.2 Experimental Methods

2.2.1 Chemicals Used

The fluorescently labelled (fluorescein and Alexa647) DNA (Table 2) were all purchased from Integrated DNA Technologies Inc. H₂AuCl₄ was purchased from Sigma-Aldrich. Milli-Q water was used for all experiments.

Table 2. Sequences of DNA used in experiments (FAM is fluorescein)

DNA	Sequence
FAM-A₁₅	5' –[6-FAM]-AAAAAAAAAAAAAAAAA-3'
FAM-G₁₅	5' –[6-FAM]-GGGGGGGGGGGGGGG-3'
FAM-C₁₅	5' –[6-FAM]-CCCCCCCCCCCCCCC-3'
FAM-T₁₅	5' –[6-FAM]-TTTTTTTTTTTTTTTTT-3'
Alexa647-A₁₅	5' –[Alexa647]-AAAAAAAAAAAAAAAAA-3'
Random 24mer	5'-[6-FAM]-ACGCATAAGAGAACCTGGG-3'
Random 24mer cDNA	5'-CCCAGGTTCTCTTATGCGT-3'

2.2.2 Gel Electrophoresis

Gel electrophoresis is an analytical technique that separates molecules based on charge distribution, mass, and shape. The principle of electrophoresis is based on the fact that electrically charged biomolecules will move freely towards the electrode of opposite charge when placed in a field of strength E . Depending on their physical traits and the experimental system used, each molecule will move at different velocities. The velocity can be described using equation 1.⁷⁵

$$v = Eq/f \quad (1)$$

q is the net charge on each molecule, v is the velocity of movement, and f is the frictional coefficient. The frictional coefficient is dependent on many factors such as mass, compactness, buffer viscosity, and porosity of the gel. For DNA, the charge distribution is particularly uniform due to the phosphate group that confers a single negative charge per nucleotide. Due to this property DNA fragments are separated due the differences in net charge and hence, the size of each fragment. The most common medium for electrophoresis to be performed in are gels. Hydrated gel networks are mechanically stable, allow post electrophoresis manipulation, and are usually chemically unreactive or minimally reactive with the biomolecules. This ensures that the molecules are separated by physical differences. The two commonly used gel types are agarose and polyacrylamide gels. Agarose gels can determine DNA molecular masses; however, they are not as mechanically stable as polyacrylamide. Polyacrylamide is much stronger and suitable for proteins and nucleic acids. It is formed by the polymerization of acrylamide cross-linked by a methylene bridge (Figure 2.1).⁷⁵

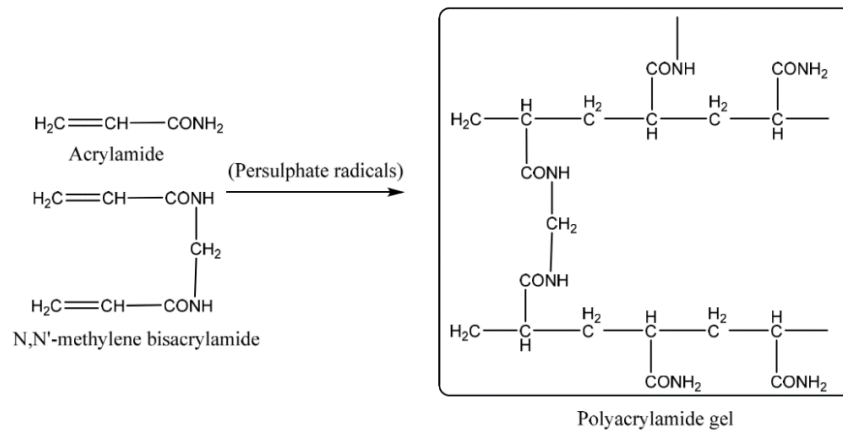


Figure 2.1 Polymerization of acrylamide, the reaction is initiated by persulphate radicals and catalyzed by tetramethylethylenediamine (TEMED). Figure adapted from Reference 75.

The gel used in these studies are a 15% denaturing polyacrylamide gel (dPAGE; denaturing polyacrylamide gel electrophoresis). This gel is denaturing due to the addition of 8M urea in the gel. The analysis of single stranded and double stranded DNA molecules can be hindered by their secondary structures. The denaturing agent unfolds the DNA by disrupting the inter-base hydrogen bonds (Figure 2.2).

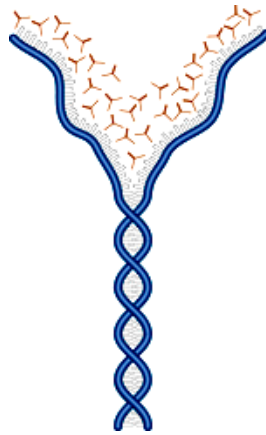


Figure 2.2 Urea denaturing the secondary structure of double stranded DNA. Figure adapted from reference 76. Copyright 2011 National Diagnostics.

Another aspect of gel electrophoresis is the loading buffer. The loading buffer usually contains something dense, such as glycerol or urea, to allow the sample to “fall” inside the wells as well as a tracking dye. These dyes migrate in the gel and allow for visual tracking of the electrophoresis progress. The dye used in the following experiments was a 1x bromophenol blue diluted in urea.

In the following electrophoresis experiments, polyacrylamide gels were prepared from a 15% polyacrylamide stock solution using TEMED (Tetramethylethylenediamine) and APS (ammonium persulfate) as polymerization catalysts. 10 μ L of the reaction mixture (including

dye) was loaded into each well. Gels were then run for 1.2 hours in 10% TBE (Tris-Borate-EDTA (ethylenediaminetetraacetic acid)) buffer at 200 V and 300 mA.

2.2.3 Fluorescence Spectroscopy

Fluorescence spectroscopy is an analytical technique that measures the fluorescence intensity of a substance containing a fluorophore. Fluorescence is produced when the fluorophore absorbs a photon of a certain wavelength which excites its electrons to a higher energy state. When this electron relaxes, it releases a photon at another wavelength which can then be detected by a fluorometer. Fluorescence readings were then taken with the Horiba Spectrophotometer with a slit width of 5 nm and an excitation and emission wavelength of 495 nm and 520 nm for FAM labelled DNA and 650 nm and 670 nm for Alexa647 labelled DNA. Reactions using FAM labelled DNA were done using pH 4 acetate buffer then put into pH 7 phosphate buffer for reading. Alexa647 labelled DNA was used for kinetics studies and the reaction was done directly in the cuvette at pH 4.

2.2.4 Buffers

Buffers used in these experiments are phosphate buffer, acetate buffer, and TBE. Phosphate has 3 pK_a values of 2.16, 7.21, and 12.32. Phosphate buffers of pH 8 and pH 6 was used in these experiments. Stock phosphate buffer was prepared at 500 mM concentration then diluted and adjusted to the correct pH using HCl and NaOH.

Acetic acid has a pK_a of 4.75. For these experiments, an acetate buffer of pH 4 was used. Similar to the phosphate buffer, a stock was prepared then diluted and adjusted to the correct pH using HCl and NaOH. TBE buffer was diluted down to working concentration from a pre-purchased stock solution.

2.3 Results and Discussion

2.3.1 A₁₅, C₁₅, G₁₅, T₁₅ DNA binding to Au³⁺

Each nucleobase has the capability to bind metal ions as shown in previous studies. As a start to studying these properties, single stranded, 5'- FAM labelled homopolymer A₁₅, C₁₅, G₁₅, and T₁₅ DNA (1 μM) were respectively incubated together with Au³⁺ ions (HAuCl₄) (90 μM) for 1 hour at room temperature. The samples were then analyzed by dPAGE. Due to the presence of 8 M urea and EDTA, the dPAGE is a rather harsh condition. Thus, if the band is shifted or disappeared, it suggested that Au³⁺ formed a very stable complex that survived the electrophoresis condition. Even though there may not be a change in band distribution in the resulting gel, there still may be a reaction with Au³⁺ but the product was not stable enough to survive the harsh denaturing conditions (high concentrations of urea and EDTA) of the gel.

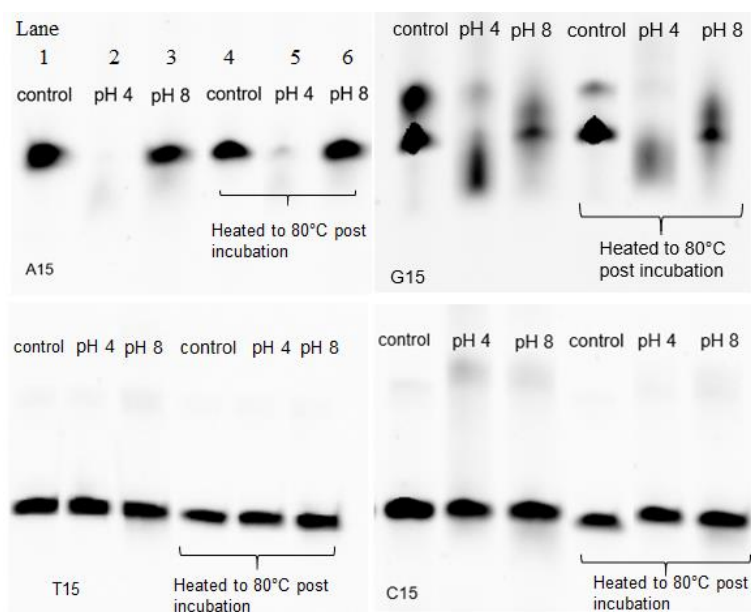


Figure 2.3 Binding of 90 μM Au³⁺ with 1 μM FAM-A₁₅ DNA, FAM-G₁₅, FAM-T₁₅, and FAM-C₁₅ DNA under low (pH 4 acetate buffer with 25 mM NaCl) and high (pH 8 phosphate buffer with 25 mM NaCl)

pH. Samples were incubated at room temperature for 1 hour then heated to 80°C for 5 minutes before loading into dPAGE.

Of the four different homopolymer DNA strands tested, only A₁₅ (Figure 2.3 top left) and G₁₅ (Figure 2.3 top right) showed a significant change in the band distribution when compared to their respective controls. C₁₅ (Figure 2.3 bottom right) and T₁₅ (Figure 2.3 bottom left) showed little if any reaction.

Starting with FAM-A₁₅, the control consisted only of FAM-A₁₅ in pH 4 acetate buffer and was a well-defined band (A₁₅ gel lane 1), which suggested that the DNA was quite pure. When the DNA and Au³⁺ ions were incubated at pH 4, there was significant quenching of the fluorophore as well as a faint band lower in the gel (A₁₅ gel lane 2). The faster migration rate could have been due to a conformation change induced by the coordination of the Au³⁺ ions to the adenine and the folding of DNA into a more compact shape. It was also notable that the structures formed by the reactions of A₁₅ and Au³⁺ were stable enough to survive both heating (A₁₅ gel lane 5) as well as being put through a denaturing gel, retaining the quenched fluorescence for imaging. However, the samples at pH 8 (A₁₅ gel lane 3,6) did not show fluorescence quenching. This could have been that the Au³⁺ ions were binding with the excess OH⁻ ions in solution. As pH increased, the formation of gold-hydroxide complexes [AuCl_(4-x)OH_x]⁻ increased.⁷⁷ The attachment of OH⁻ ions to the gold center could have possibly interfered with the binding to adenine bases. The excess amounts of OH⁻ ions could have also affected the electrostatic activity between the Au³⁺ and DNA. Because there was no quenching observed did not mean that there was no reaction, but that any formed complexes were not stable enough to remain through heating or the denaturing gel.

G₁₅ was also seen to have reactions with Au³⁺. However, unlike A₁₅, the control band of G₁₅ was not one well defined band but two bands with the first band above the second (G₁₅ gel lane 1). Poly-G DNA is known to form secondary structures with itself, such as dimers or quadruplex DNA. This upper band also dropped in fluorescence significantly upon heating leading to the conclusion that the structures formed were not as stable. Upon the addition of gold, smearing of the bands was observed similar to the bands in A₁₅. G₁₅ retained more of the fluorescence in the lower band at pH 4 but the upper band was very faint (G₁₅ gel lane 2). The lower band also travelled further down the gel similar to the complex with adenine at pH 4. However, there was significantly more fluorescence intensity in G₁₅. Although the Au³⁺ could be binding to G₁₅ in a similar fashion to A₁₅, the resulting structure was not stable enough to go through denaturing and fluorescence was recovered. Au³⁺ had been found to bind guanine previously, but the resulting structure is very unstable in solution and the gold could have oxidized the purine ring.⁶³ Upon heating, the pH 4 sample (G₁₅ gel lane 5) more closely resembled A₁₅, however, due to the necessity of heating, the overall stability of the Poly-G-Au³⁺ complex was questionable. In the pH 8 sample (G₁₅ gel lane 3,6), the band positions were different from the sample at pH 4 but similar to the control. However, there was no band lower in the gel, just the two bands at a similar position to the control. This could mean that at higher pH, the gold was not reacting with the DNA to the degree seen at pH 4. After heating there was more intensity in the lower band of the control (G₁₅ gel lane 4) most likely due to the breaking apart of secondary structures by heating.

T₁₅ DNA showed no change in the band distribution from the control. This was not surprising since thymine has the lowest affinity for metal ions and usually only one available

binding site. However, reactions may still have occurred but were not stable enough to survive electrophoresis conditions.

C₁₅ DNA also did not seem to have any reactions with Au³⁺. There was a faint upper band in the control (C₁₅ gel lane 1), pH 4 (lane 2), and pH 8 (lane 3). However, this band disappeared upon heating (C₁₅ gel lanes 4,5,6). This could have been due to the fact that C- rich DNA can form secondary structures, such as the i-motif. i-motif DNA is usually most stable at pH 5 – 6, which is close to pH 4. If this was not the i-motif forming, the Au³⁺ could have been crosslinking some of the C₁₅ DNA, but these structures were not very stable as they completely disappeared upon heating.

The above analyses used fluorescence quenching as the method of determining whether any reaction or complexation happened between the DNA and the Au³⁺. Hence, a discussion of possible quenching mechanisms would prove helpful in understanding these reactions.

The covalently bound Au³⁺ acts as a fluorescence quencher. There are two possible mechanisms of fluorescence quenching for the scenarios above. These two are an energy transfer or an electron transfer. Fluorescence occurs when electrons in the fluorophore are excited to a higher energy by an incident wavelength. The photon released upon relaxation back to ground state is what we then observe as fluorescence. Each fluorescent material usually has an absorption wavelength and an emission wavelength. In the case of quenching by energy transfer, there usually needs to be an overlap between the absorption spectrum of the quencher and the emission spectrum of the fluorophore. So, the energy released by the fluorophore is absorbed by the quencher. This then results in a reduced fluorescence lifetime and less fluorescence is observed. This type of fluorescence quenching is unlikely for the systems described above. This is due to the lack of spectra overlap between fluorophore (FAM) and the quencher (Au³⁺). The

form of Au^{3+} used in the reactions ($[\text{AuCl}_4]^-$) has been seen to absorb at 313 nm⁷⁷ while the emission wavelength of the FAM label is around 520 nm. Therefore, there is no overlap making this an unlikely mechanism for quenching.

The second possible quenching mechanism, an electron transfer, is the more likely case in this scenario. An excited electron can be transferred to the attached gold due to the conformation change brought about by the complexation of the Au^{3+} and the DNA. This results in a no fluorescence at all, which was seen in the A_{15} gels.

2.3.2 Binding of Au^{3+} by A_{15} as a function of Salt

The previous study showed that A_{15} DNA and Au^{3+} ions had the ability to form a very stable complex. Since Au^{3+} was initially complexed with Cl^- , and the affinity between Au^{3+} and halides follows the rank of $\text{F}^- < \text{Cl}^- < \text{Br}^- < \text{I}^-$, it would be interesting to see the reaction between DNA and Au^{3+} with different ligands. To get a better idea of these interactions, Au^{3+} and A_{15} DNA were further studied through varying the salt concentration and type.

Factors that affected binding such as salt concentration, temperature, pH and competition with other molecules were studied. As seen previously, the pH at which the reaction took place was an important factor in the study of this binding. The binding clearly favored a lower pH in order to take place, seeing almost no change in band distribution at higher pH levels possibly due to the interference of increasing levels of OH^- .

Salt, in this case sodium chloride (NaCl) was added to the reaction buffer to stabilize charge on the DNA strands, thus reducing electrostatic repulsion and increasing binding. Without some type of salt, there was very little covalent binding of Au^{3+} to the DNA (Figure 2.4, 0 mM

salt). The effects of different salts on the complexation of Au^{3+} and FAM- A_{15} DNA can be seen in Figure 2.4 and 2.5.

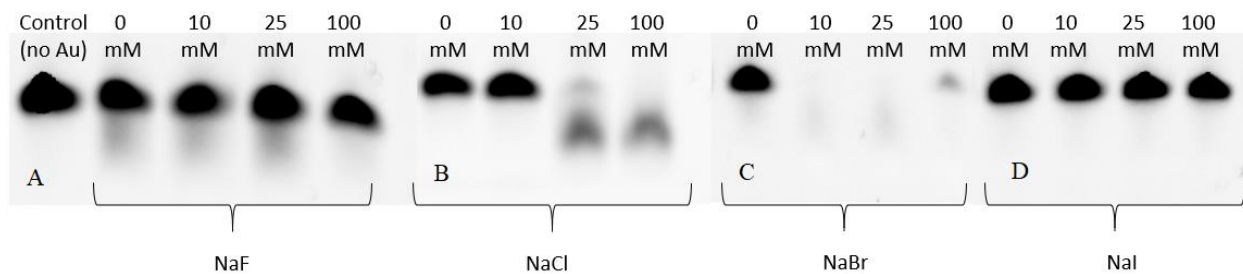
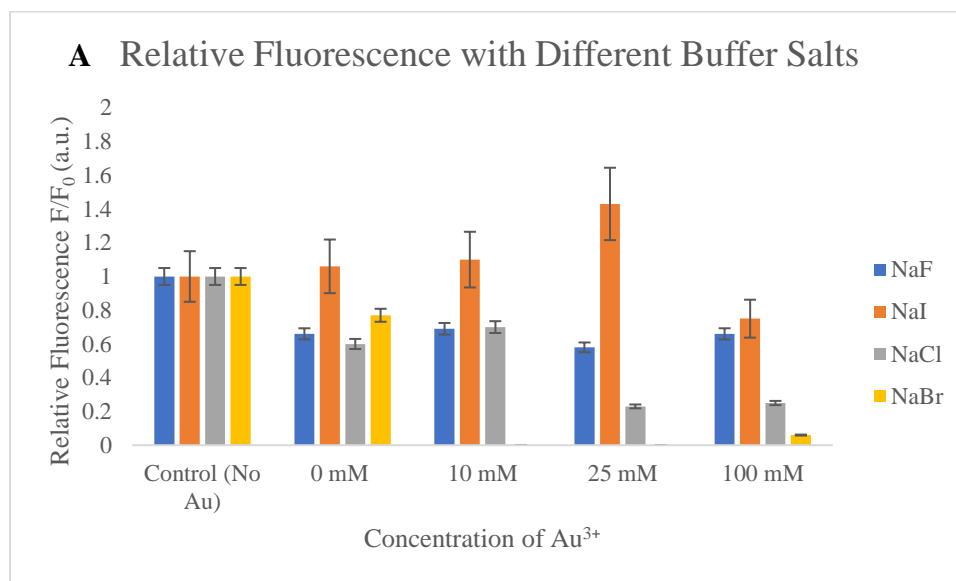


Figure 2.4 Effect of different salts at different concentrations. Samples contain $90 \mu\text{M Au}^{3+}$ and $1 \mu\text{M A}_{15}$ DNA incubated for 1 hour at pH 4 acetate buffer. Each salt was added to the buffer prior to incubation to obtain the noted concentrations.



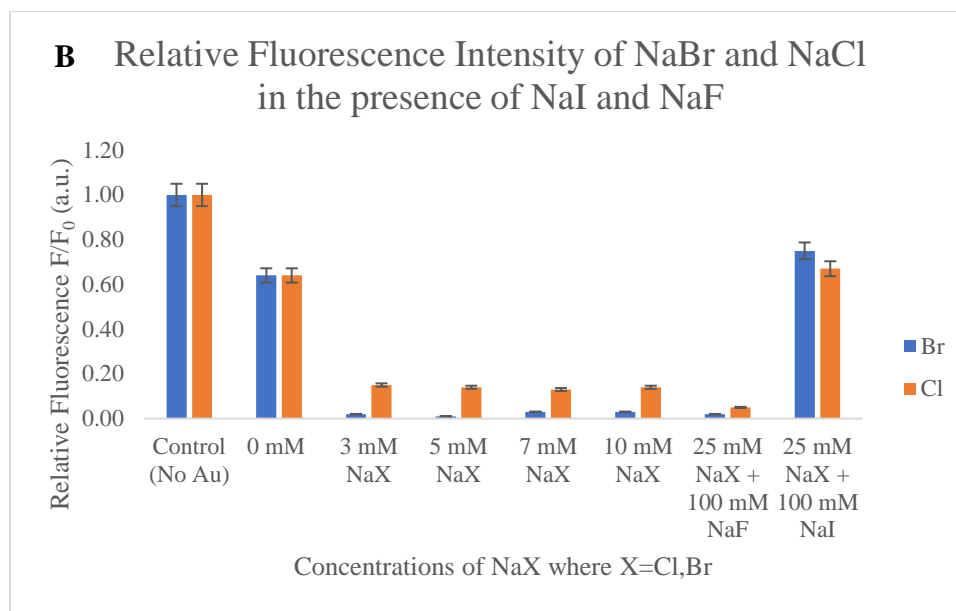


Figure 2.5 A) Relative fluorescence intensity post-electrophoresis of different buffer salts B) comparison of NaCl and NaBr buffer salts

The state of gold in the reaction was not naked Au^{3+} but bound to other atoms. The original source of Au^{3+} was HAuCl_4 , therefore the Au^{3+} originally existed in solution as $[\text{AuCl}_4]^-$ with the possibility of small amounts of AuCl_3 . While the cation of the salt provides the charge screening necessary for the interaction of the Au^{3+} and DNA, the anion may affect this initial gold structure by replacing one or more of the Cl^- to form new complexes before binding to DNA (Figure 2.6).

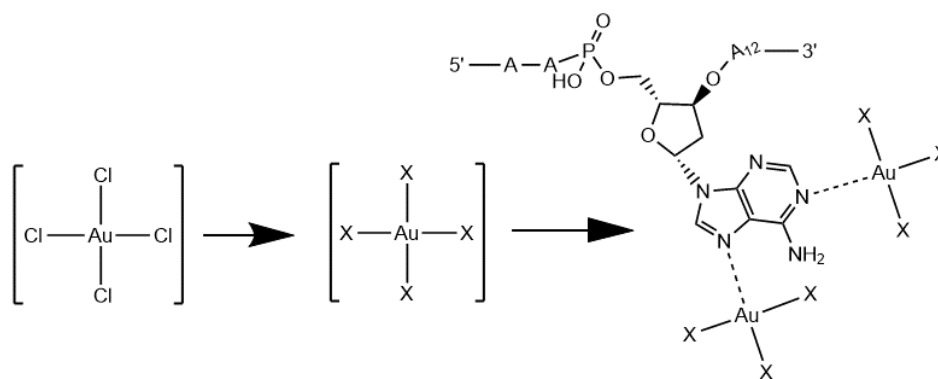


Figure 2.6 A possible scheme for Au³⁺ binding with adenine in A₁₅. Since Au³⁺ comes from HAuCl₄, it first exists in solution at [AuCl₄]⁻. Upon the addition of other reagents, one or more Cl⁻ can be replaced by other ligands to form [AuCl_(4-y)X_y] based on affinity before binding to N1 or N7 sites on the adenine bases in the DNA (X= F⁻, Cl⁻, Br⁻, I⁻, OH⁻)

First, sodium fluoride was used as the buffer salt. The binding in the NaF gel was similar to having no salt at all (Figure 2.4A). This was not unexpected since F⁻ has the lowest affinity for gold and would not replace any of the initial Cl⁻ in [AuCl₄]⁻. Although the buffer with NaF may have had some binding, it was most likely noncovalent and did not survive denaturation. Iodide also showed no quenching (Figure 2.4D). Iodide has the highest affinity for gold⁷⁸ (Table 3) and would easily replace the Cl⁻. Due to this high affinity, the iodide was not easily removed by the DNA and thus no complexation with the DNA was seen.

Table 3. Formation constants with Au³⁺.

X ⁻	β_4 (Au ³⁺)
Cl ⁻	1x10 ²⁶
Br ⁻	1x10 ³²
I ⁻	5x10 ⁴⁷
CN ⁻	~10 ⁵⁶

Chloride and bromide did show signs of facilitating complex formation. At concentrations above 25 mM for NaCl (Figure 2.4B) and 10 mM of NaBr (Figure 2.4C), there was quenching of the fluorophore indicating the formation of the Au-A₁₅ complex. Interestingly, the reaction in the presence of Br⁻ appeared to be more complete than with Cl⁻. Although, Br⁻ has a higher affinity for gold, it may be more readily removed by the DNA or by allowing the conformation change to bring the gold closer to the FAM label, resulting in more quenching. However, there seemed to be a threshold for Br⁻ since the fluorescence is coming back at 100 mM NaBr. Br⁻ being a better

catalyst when compared to Cl^- for such activity has also been reported in gold nanoparticle conjugation where it showed higher DNA adsorption in the formation of AuNP-DNA conjugates.⁴⁰ NaI and NaF were added in addition to NaCl and NaBr (Figure 2.5B) to see what effect these had on the ability of Cl^- and Br^- to facilitate binding. Samples with NaF showed similar binding to samples without NaF, but samples including NaI showed very little change in fluorescence. These can confirm that there might have been a switching of ligands attached to Au^{3+} before binding with the DNA and that not all the Cl^- initially attached to the Au^{3+} center is replaced. It is more likely that only some are replaced since there is still a slight drop in intensity when NaI was used.

2.3.3 Stable Binding of Au^{3+}

The selectivity of Au^{3+} for polyadenine DNA was tested by comparing pure A_{15} DNA to a random DNA strand with a sequence of 24 random bases. Two additional metals, lead (Pb^{2+}) and mercury (Hg^{2+}), were used for comparison. Hg^{2+} is isoelectronic to Au^{3+} and Pb^{2+} is a heavy metal atom (Figure 2.7).

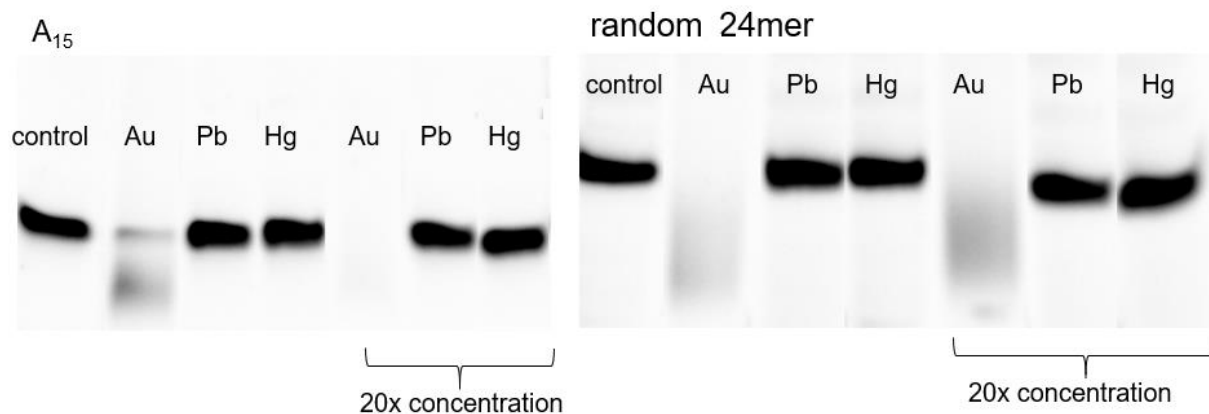


Figure 2.7 Binding of gold, lead, and mercury ions ($90 \mu\text{M}$ and 1.8 mM) to A_{15} and a random 24mer DNA ($1 \mu\text{M}$) in acetate buffer (pH 4 with 25 mM NaCl)

Pure FAM-A₁₅ DNA showed no reaction with Hg²⁺ and Pb²⁺ under the same conditions even though Hg²⁺ has a similar capacity to bind halides. For comparison, metal concentrations of 20 times higher were also tried. The binding of Au³⁺ and A₁₅ DNA were very selective for each other. There was no change in the band distribution from the control in both the lead and mercury samples whereas there was very clear smearing and fluorescence quenching in the A₁₅ samples. Even at 20 times the metal concentration, there was still no change in band distribution for lead and mercury. In the random 24mer, the reaction between the DNA and the Au³⁺ may also involve coordination and binding to the guanine bases as well. As seen before, the Au³⁺ also binds to guanine bases and formed less stable complexes.

The complementary DNA (cDNA) to the random 24mer DNA used previously was incubated with Au³⁺ ions to study the effect of a competitor molecule as well as the effect on double helix formation (Figure 2.8).

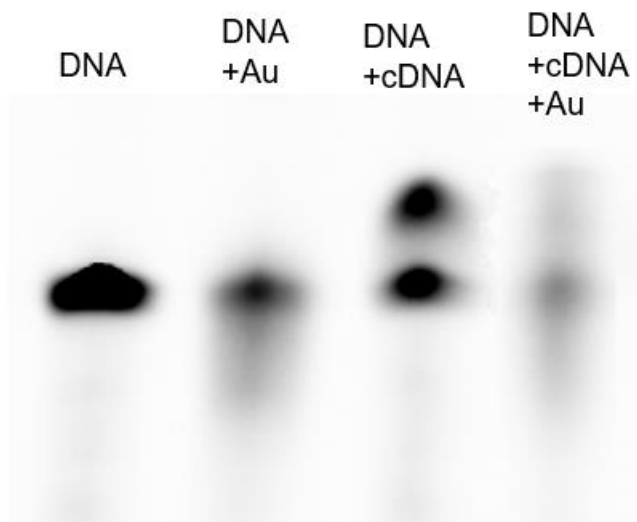


Figure 2.8 Effects of gold on complementary DNA (cDNA)

There was both band smearing and fluorescence quenching when both cDNA and Au³⁺ were added. Both were added at the same time and allowed to incubate for 1 hour at room

temperature. Compared to the cDNA+DNA lane, when Au^{3+} was added, there is still a faint band where the duplex was formed. Although this band was very faint, this could mean that the duplex DNA was still forming and the Au^{3+} was perturbing, but not completely destroying the binding of the nucleobases.

2.3.4 Fluorescence Studies

Fluorescence spectroscopy was used to monitor binding kinetics in real time. Also, the conditions for fluorescence spectroscopy were not as harsh as dPAGE, hence any reactions that would have been destroyed by electrophoresis could be observed. Fluorescence studies were conducted with both Alexa and FAM labelled DNA. Binding was studied as a drop or decrease in the fluorescence signal.

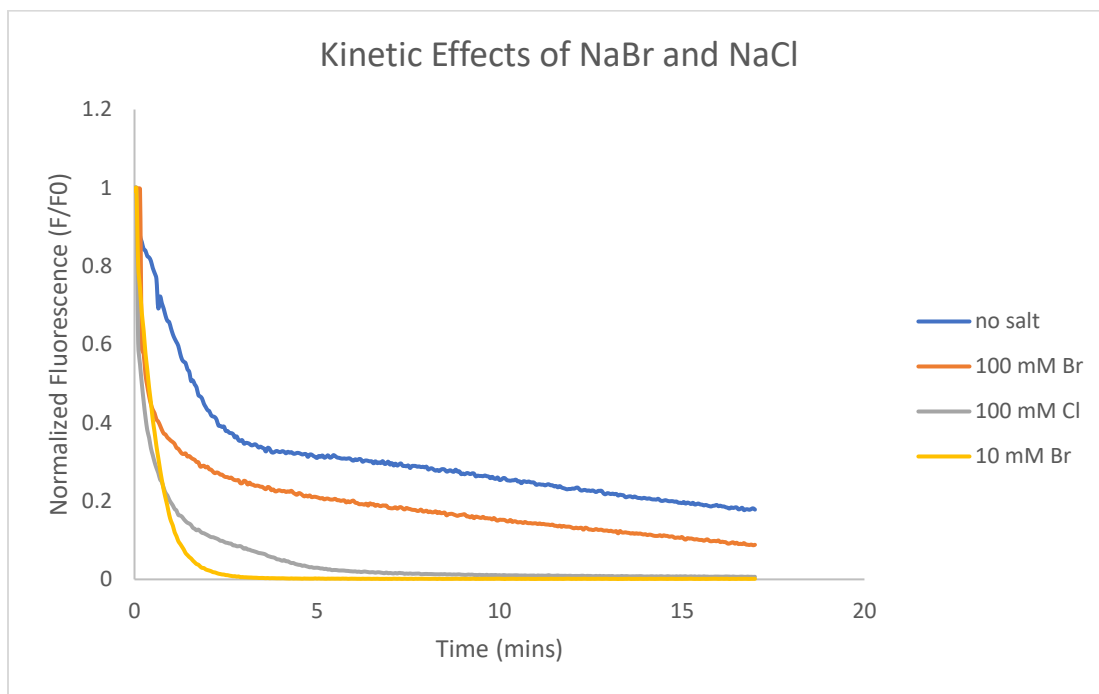


Figure 2.9 Kinetic effects of using NaCl and NaBr as buffer salts in pH 4 acetate buffer

Table 4. First order rate constants. Fit to $F = F_0 + a(1 - e^{-kt})$.

Salt Concentration	k_{obs} (mins ⁻¹)	R ² -value
No Salt	0.60	0.9518
100 mM NaBr	0.91	0.8204
100 mM NaCl	1.5	0.9187
10 mM NaBr	1.9	0.9982

The kinetics of the reaction were plotted in Figure 2.9 with variations in the buffer salt. The reaction was then fitted to first order rate constants (Table 4). The samples that contained no salt were clearly very slow to react completely. Without the addition of salt, the binding of Au³⁺ to the DNA was most likely not covalent and was easily destroyed upon heating and denaturing. By adding NaCl and NaBr, the rate constant went up. Similar to the gel results, at 10 mM of NaBr, the reaction went to completion much faster ($k = 1.9 \text{ mins}^{-1}$) than 100 mM NaCl ($k = 1.5 \text{ mins}^{-1}$) with more of the DNA being quenched. In addition to increasing the rate constant, the sample with 10 mM NaBr also showed a much steeper drop in the beginning indicating that the Br⁻ promoted faster binding than the Cl⁻. The reaction rate also went down at 100 mM NaBr, matching the gel studies. Although reaction kinetics were modelled as first order, there are possible complications. The exact number of Au³⁺ that could bind to each A₁₅ DNA is still unknown. If the binding was not 1:1, the effect of additional Au³⁺ binding to the same DNA strand and the effect that had on the degree of fluorescence quenching should be studied further.

Some of this can be seen in Figure 2.9. Other than the 10 mM NaBr sample, the other samples showed somewhat two-phase reaction kinetics. There was an initial fast decrease of

fluorescence up until around 4 minutes. Past this point, the fluorescence continued to drop but at a slower rate. One possibility is that as each A₁₅ strand was getting more saturated with Au³⁺, the previously bound Au³⁺ ions were inhibiting the further binding of more Au³⁺. Another possibility is that the Au³⁺ was acting as a quencher for more than one strand of A₁₅. After saturating one strand of A₁₅, the Au³⁺ could crosslink with other strands of DNA that still had sites available for binding.

2.3.5 Fluorescence Recovery

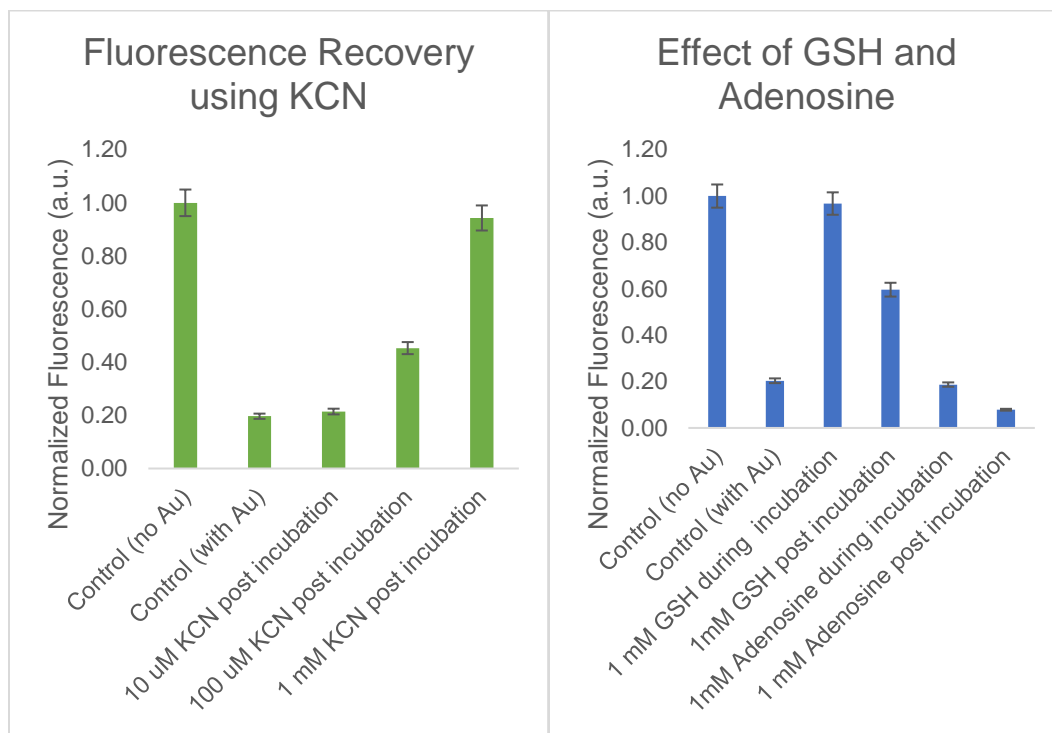


Figure 2.10 Fluorescence recovery using potassium cyanide (KCN), glutathione (GSH), and free adenosine

Potassium cyanide (KCN), glutathione (GSH) and free adenosine were added to samples post incubation to try to disrupt the binding and recover the fluorescence (Figure 2.10). The CN⁻ has a very high affinity for Au³⁺ (Table 3) and could easily remove the gold from the DNA. The

fluorescence signal increased with the concentration of KCN added to almost complete recovery at 1 mM KCN. GSH also recovered fluorescence when added post incubation. However, when added during incubation, the GSH almost completely inhibited the binding between A₁₅ DNA and Au³⁺ ions. Au³⁺ is highly thiophilic and has a much higher affinity for thiols than the nucleobases and was most likely binding to the thiol group in GSH. Therefore, when added during incubation, the DNA could not out compete the Au-S binding of the GSH. The free adenosine had little to no effect on the binding. This showed that although the DNA has a faster migration rate, the fact that fluorescence could be recovered suggests that this interaction is reversible binding as opposed to irreversible cleavage.

2.4 Conclusions

The binding properties of fluorescently labelled A₁₅ DNA and Au³⁺ ions were studied using gel electrophoresis and fluorescence spectroscopy. When compared to other fluorescently labelled homopolymer DNA (C₁₅, T₁₅, G₁₅), A₁₅ was the only one that showed a clear binding and coordination of Au³⁺ through the quenching of the fluorophore. Further studies were aimed at the formation and stability of the Au³⁺ - A₁₅ complex. Complex formation of Au³⁺ and A₁₅ favored a lower pH environment compared to a higher pH environment. The formed complex was stable enough to survive the addition of a denaturing agent, urea, as well as post incubation heating to 80°C and dPAGE conditions. Salt was found to be necessary to reduce long distance charge repulsion and was equally important in facilitating the binding of A₁₅ to Au³⁺ and complex formation. Out of 4 sodium salts (NaF, NaCl, NaBr, NaI) only two of the salts (NaCl and NaBr) showed evidence of complex formation. Interestingly, the addition of Br⁻ showed a larger drop in fluorescence as opposed to Cl⁻, contrary to established trends. The concentration of Br⁻ and Cl⁻ also affected rate of reaction with 10 mM Br⁻ showing faster reaction speed than 100

mM Cl⁻ but 100 mM Br⁻ showed a decrease in reaction which agrees with the fluorescence observed in the gel electrophoresis studies. First order reaction rate constants were found to be 0.60 mins⁻¹, 0.91 mins⁻¹, 1.5 mins⁻¹, and 1.9 mins⁻¹ for buffers with no salt, 100 mM NaBr, 100 mM NaCl, and 10 mM NaBr respectively.

Moving forward from purely single base DNA sequences, this binding was observed using a random sequence of 24 bases. In the presence of other bases and metal ions, the Au³⁺ ions were still solely coordinated by the DNA strand showing that the binding sites in adenine have a very high affinity for Au³⁺. The complement of the random 24mer DNA was also looked at for competition with Au³⁺. The cDNA was unable to hybridize with the 24mer in the presence of Au³⁺ leading to the conclusion that the gold out competes the cDNA for binding and the resulting complex does not allow complete hybridization.

As strong as this binding was, it was not irreversible. Fluorescence was able to be recovered. Fluorescence recovery was tested with three reagents, potassium cyanide (KCN), glutathione (GSH) and free adenosine. KCN and GSH were able to effectively recover a fluorescence signal after complex formation. KCN was able to almost completely recover the fluorescence while GSH recovered about 60% when added post incubation. The adenosine was not able to recover the fluorescence.

This strong binding has many implications on possible applications. First, the hybridization of DNA strands is greatly inhibited in the presence of Au³⁺. Depending on the system being studied, this property could present an obstacle when trying to hybridize any DNA containing adenine bases. The DNA would likely be unable to bind any other substances. The presence of Au³⁺ will also affect the properties of other functional DNA (aptamers, DNazymes, etc) by out competing other substrates and disrupting the intended effects.

Chapter 3 - Effect of Au³⁺ on DNAzyme activity

3.1 Introduction

The notion for using DNA as possible biosensors first came about in the early 1990s when scientists first developed a method for selecting RNA (ribonucleic acid) sequences that could bind to target molecules.⁷⁹ These oligonucleotide sequences were then named aptamers, derived from the Latin *aptus* meaning “to fit”. Following these RNA aptamers, DNA aptamers were also discovered.⁸⁰ Due to their unique properties, aptamers have become very popular molecular tools for therapeutic and diagnostic applications. First, the target for aptamer binding can vary greatly from small molecules to large proteins, depending on the binding specificity, thus giving aptamers a wide range of biosensing applications.⁸¹ DNA aptamers can also be reproduced with high purity and are usually very chemically stable. Finally, aptamers can undergo conformational changes upon target binding and can offer sensors with high sensitivity and selectivity.⁸¹ Aptamers have been found to aid in the detection of bacteria such as *Staphylococcus aureus*,⁸² as well as being able to functionalize the surface of both silver and gold nanoparticles.^{83,84}

The word DNAzyme comes from a combination of DNA and enzyme. It has been shown that many DNA molecules can catalyze a variety of reactions in a manner similar to enzymatic activity. The reactions that DNAzymes can catalyze are very similar to the reactions catalyzed by RNAzymes(ribozymes) such as cleavage of DNA/RNA, ligation, phosphorylation, cleavage of phosphoramidate bonds, and porphyrin metalation.⁸⁵ However, in order for DNAzymes to be effective in its applications, they must be able to compete with other catalysts for efficiency and diversity. Due to the structural limitations of DNAzymes (only 4 nucleobases available) and the absence of the 2'-OH(compared to RNAzymes), cofactors have been employed to overcome

these limitations; the most popular being metal ions.^{85,86} Divalent metals such as magnesium, zinc, and calcium ions play a vital role in the catalytic function of DNazymes.

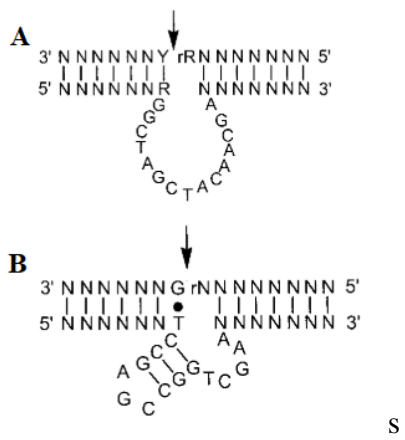


Figure 3.1 Examples of DNazymes **A)** “10-23” DNzyme with RNA cleaving activity **B)** “8-17” DNzyme with RNA cleaving activity. Figure adapted from Reference 85.

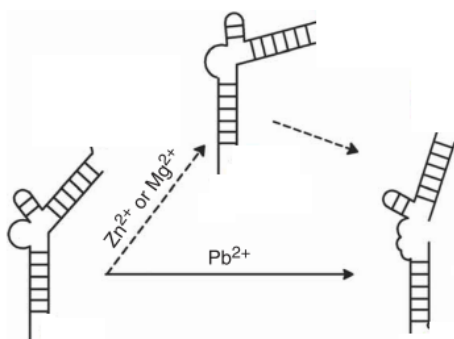


Figure 3.2 Cleavage action of 17E DNzyme on a substrate catalyzed by metal ions. Figure adapted from Reference 86. Reprinted by permission from Springer Nature Customer Service Centre GmbH : Springer Nature, Nature Chemical Biology Kim, H.-K., Rasnik, I., Liu, J., Ha, T. & Lu, Y. Dissecting metal ion-dependent folding and catalysis of a single DNzyme., 2002.

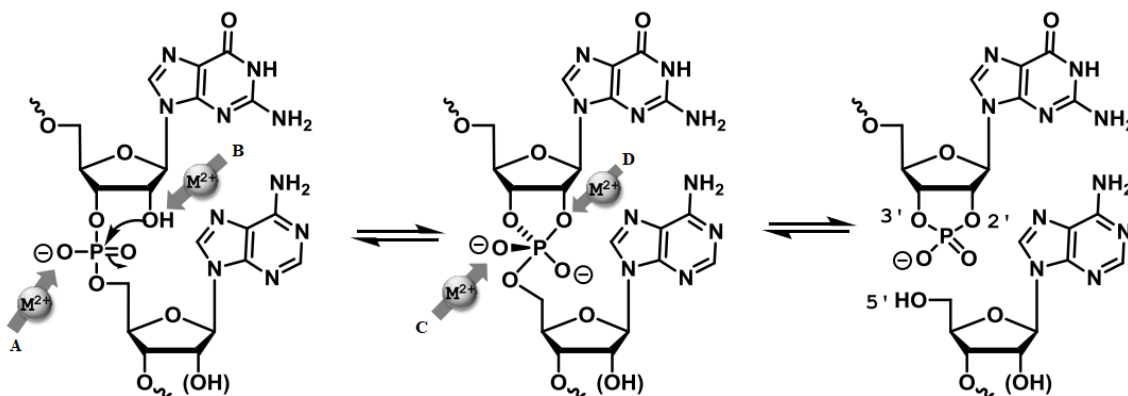


Figure 3.3 Possible mechanism of DNAzyme cleavage. **A)** negative charge stabilization of oxygen atom, **B)** activation of the nucleophilic hydroxyl by deprotonation or coordination, **C)** stabilization of the negative charge built-up on the oxygen of the leaving group, **D)** general base catalysis. Figure adapted from reference 87.

The folding of the DNAzyme induced by divalent metals allows the positioning of the substrate and the functions involved in the catalytic step. The divalent metal ion will then activate the nucleophilic 2'-hydroxyl group. This leads to a nucleophilic attack on the phosphorus center which leads to the pentavalent intermediate that is then broken down into a 2',3'-cyclic phosphate and 5'-OH products (Figure 3.3).⁸⁷

DNAzymes have become widely used as detectors and sensors. Some examples include a mercury sensor made from the 10-13 DNAzyme (Figure 3.1A)⁸⁸ and a lead sensor using the 17E DNAzyme (Figures 3.1B and 3.2).⁸⁹

Both DNA aptamers and DNAzymes have been known to interact with metal ions. In the case of DNA aptamers, these interactions have been studied for the detection of metals such as lead and mercury ions.^{90,91} As previously mentioned, divalent metal ions are essential for the catalytic function of DNAzymes. Both interactions are based on the complexes and chemical

reactions formed by the reactions and coordination of the metallic ions and the individual nucleic acids that make up the aptamer or the DNAzyme.

In the previous chapter, the very strong binding of Au³⁺ and adenine DNA was studied. These interactions have the potential to disturb the functions of DNAzymes and could affect the cleavage rate and efficiency. The effects of Au³⁺ on the activity of DNAzymes has not been well studied before. Since the 17E DNAzyme is well studied and known to have good cleavage action, it was used in the following studies as a model to see the effect of Au³⁺ ions on the cleavage activity of DNAzymes.

3.2 Experimental

3.2.1 DNAzyme preparation

The 17E DNAzyme and PO substrate (Table 5) were purchased from Integrated DNA Technologies Inc.

Table 5. Sequences of 17E and PO substrate

Name	Sequence (5' – 3')
17E DNAzyme	CAGTGCTCAGTGATAAAGCTGGCCGAGCCTCTTCTACCGC
Substrate (PO)	FAM-TCAGACCTAGGAAGTTGCAGTACTCCGCTTGC

The DNAzyme and substrate were first annealed together to form a duplex. 17E and PO were mixed together in 10 mM of pH 6.0 MES(2-(*N*-morpholino) ethanesulfonic acid) buffer with 25 mM NaCl. This solution was then heated to 95°C for 1 minute then slowly cooled to 4°C for 30 minutes in a thermal cycler.

3.2.2 Activity assay

This working solution of DNAzyme and substrate was then combined with a zinc catalyst (ZnCl_2) and other experiment reagents in 10 mM pH 6.0 phosphate buffer with 25 mM NaCl and incubated for 1 hour at room temperature. After incubation, dye containing 8M urea was added and samples were loaded into a denaturing polyacrylamide gel then run for 1.2 hours at 200 V and 300 mA.

Electrophoresis bands were then quantified based on relative fluorescence intensity. The percentage cleaved was calculated using Image Lab software as band percentage. Total lane intensity was calculated as intensity of cleaved product (lower band) + intensity of uncleaved duplex (upper band) in each lane.

3.3 Results and Discussion

3.3.1 DNAzyme activity in the presence of Zn^{2+}

To understand the effect of Au^{3+} , we chose to study the 17E DNAzyme. To follow its cleavage activity, the substrate strand was labeled with a FAM fluorophore. The enzyme strand was then hybridized with the substrate strand to form the DNAzyme complex. Before studying the effect of Au^{3+} on the cleavage ability of the 17E DNAzyme, the activity of the DNAzyme in the presence of Zn^{2+} was tested first, and denaturing gel electrophoresis was once again used to follow the cleavage activity.

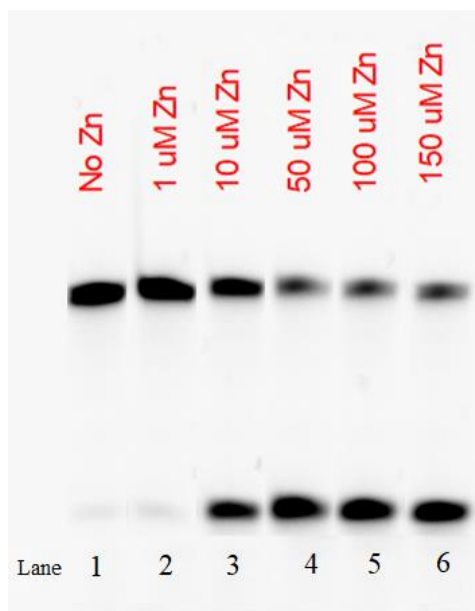


Figure 3.4 The cleavage action of 17E with regards to Zn²⁺ concentration

If the DNase I was active, then a short product was produced that migrated faster down the gel (Figure 3.4). Without the addition of Zn²⁺ into the DNase I complex (substrate plus enzyme), no cleavage was observed (lane 1). The cleavage ability of the 17E enzyme increases with increasing concentration of Zn²⁺ (lanes 2-6) and peaked at around 71% cleavage with 100 μ M Zn²⁺. This indicated that the cleavage required both the enzyme strand and Zn²⁺, consistent with the literature.⁹²

3.3.2 Effect of soft metal ions on the activity

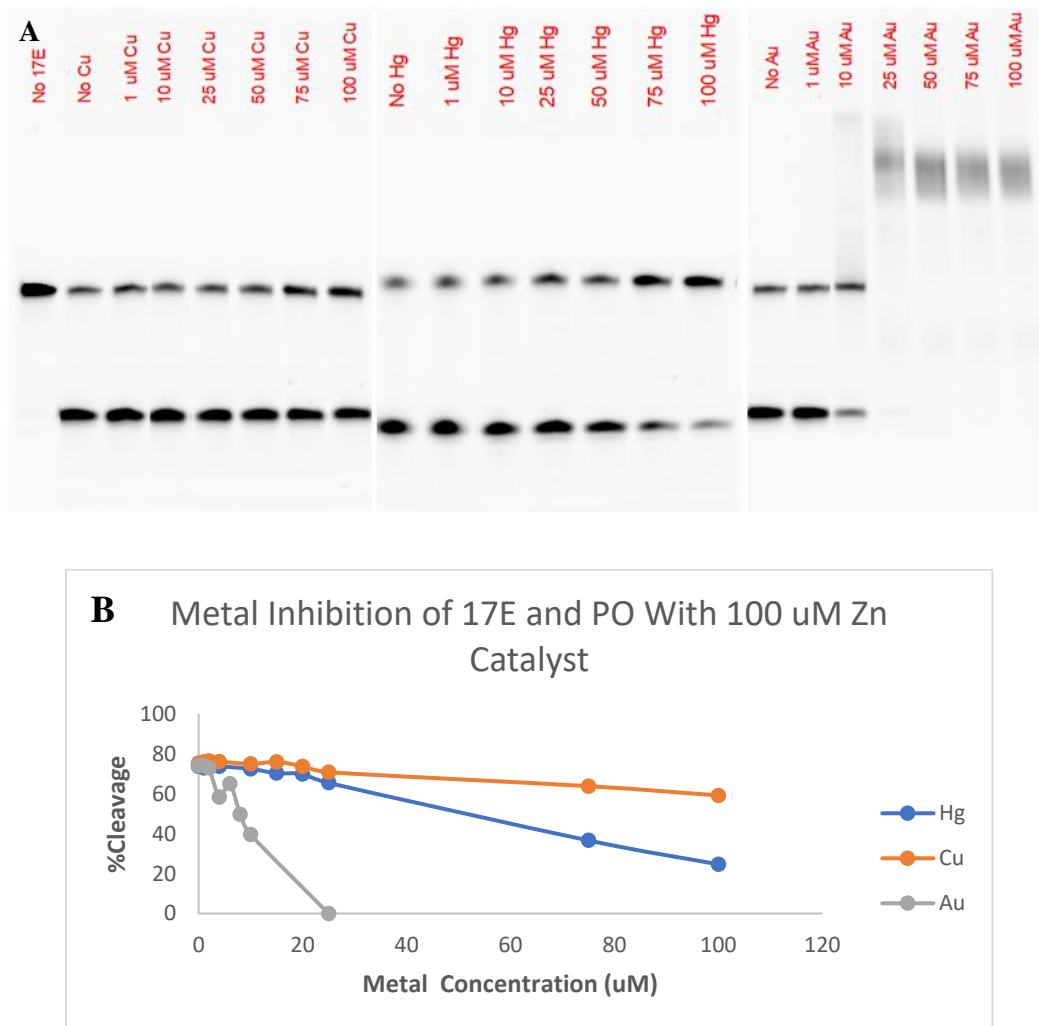


Figure 3.5 A) The effects of Au^{3+} , Hg^{2+} , and Cu^{2+} ions on the action of 17E B) A graph quantifying the drop in cleavage

The effect of other metal ions in addition to Zn^{2+} were then studied. Without the addition of any additional metal ions, the DNAzyme cleaved the substrate very well, increasing the percent cleaved with increasing concentration of Zn^{2+} (Figure 3.3). In addition to Au^{3+} two other metals were tested for comparison, Hg^{2+} and Cu^{2+} (Figure 3.5A) and their effects on the percentage of substrate cleaved were summarized (Figure 3.4B). While Hg^{2+} dropped cleavage

to 30%, Cu^{2+} had very little effect on the cleavage ability of the 17E DNAzyme. However, there was a clear inhibition of activity for concentrations of Au^{3+} 25 μM and greater.

Binding activity of Au^{3+} was indicated by the change in total fluorescence intensity of each lane. Total lane intensity remained constant for Cu^{2+} and Hg^{2+} , however the lane intensity dropped to 62% of its original intensity when going from 10 μM Au^{3+} to 25 μM Au^{3+} . Band smearing was also observed and used as evidence of binding occurring.

There was a similarity to the smeared bands observed in the reaction of polyadenine and Au^{3+} , however these smeared bands were much higher in the gel. This indicated that the Au^{3+} ions were binding to the duplex formed by the DNAzyme and PO substrate. This smearing was higher than the uncleaved bands suggesting that the gold could have possibly been crosslinking the 17E-PO duplexes to form larger structures that survived denaturation. These complexes were then unable to bind with the Zn^{2+} necessary to catalyze the reaction.

3.3.3 Discussion

Three different metal ions were compared for their reactions with the 17E DNAzyme. Au^{3+} , Hg^{2+} , and Cu^{2+} were added to the DNAzyme-substrate duplex and were studied in terms of inhibition and stability. Cu^{2+} had almost no effect on the cleavage ability. Hg^{2+} showed some inhibition, dropping the cleavage percentage down to around 30%. Au^{3+} had the most inhibitory effect as there was no cleavage past 25 μM . Au^{3+} also formed the most stable complex, able to survive denaturing electrophoresis. Complexation is shown by the smearing of bands, similar to the reaction with A_{15} DNA. The higher position of the bands suggests that Au^{3+} was able to crosslink the DNAzyme-substrate duplex. Since this behavior was observed in both the A_{15} and the DNAzyme experiments, gold could be a useful chemical for the stable crosslinking of DNA strands.

Through the study of these interactions, it is clear that attention needs to be paid to Au^{3+} when working with DNA or doing DNA based assays, not only when using DNAzymes, but all sorts of DNA aptamers or DNA probes. Au^{3+} is very likely to interfere with the performance of the DNA.

3.4 Conclusions

Based on the previous studies of complexation between A_{15} DNA and Au^{3+} ions, the impact of these interactions on the cleavage activity of the 17E DNAzyme was studied. Under normal conditions, the 17E DNAzyme cleaved an RNA substrate in the presence of a Zn^{2+} catalyst. Without the addition of other metal ions, 17E had a cleavage percentage of 71% with 100 μM of Zn^{2+} . In addition to Au^{3+} , Hg^{2+} and Cu^{2+} ions were also tested. Au^{3+} showed the most inhibitory effect, completely deactivating the DNAzyme at concentrations of 25 μM . Both Hg^{2+} and Cu^{2+} showed a much less inhibitory effect with Hg^{2+} dropping the cleavage to around 30% and Cu^{2+} doesn't not seem to have an effect. The higher position of the smeared bands in the presence of Au^{3+} suggests that the gold is interacting with the 17E-PO duplex, possibly crosslinking to construct larger structures.

Chapter 4 - Conclusions and Future Work

4.1 Conclusions

The interactions between gold ions (Au^{3+}) and DNA were studied using FAM and Alexa labelled DNA in combination with techniques such as gel electrophoresis and fluorescence spectroscopy. From the gel electrophoresis studies, C_{15} and T_{15} DNA did not show any notable interactions with Au^{3+} ions. G_{15} showed some reactions indicated by different band distributions, however the complexes formed by the G_{15} were not stable under denaturing conditions. A_{15} DNA showed the highest activity with Au^{3+} , forming a stable complex that survived harsh dPAGE conditions.

The complexation of A_{15} DNA and Au^{3+} ions was found to be pH dependent and favored a lower pH (pH 4) over a higher pH (pH 8). The complex was also strong enough to endure post incubation heating as well as a denaturing gel. This binding may have also caused a conformational change in the DNA itself, evidenced by the bands being lower in the gel than the control. The binding of the A_{15} DNA and Au^{3+} could be disrupted and the fluorescence was able to be recovered by potassium cyanide (KCN) and glutathione (GSH) but not adenosine.

The effects of salt on the formation of the $\text{A}_{15} - \text{Au}^{3+}$ complex was studied using four different salts (NaF, NaCl, NaBr, and NaI). No complex formation was observed when NaF or NaI was used as a buffer salt. However, both NaCl and NaBr facilitated the formation of the complex. First order kinetic rate constants were determined to be 0.60 mins^{-1} , 0.91 mins^{-1} , 1.5 mins^{-1} , and 1.9 mins^{-1} for complex formation with no salt, 100 mM NaBr, 100 mM NaCl, and 10 mM NaBr respectively. Lower concentrations of NaBr showed faster binding of DNA and Au^{3+} when compared to NaCl, but higher concentrations of NaBr slowed down the reaction.

This interaction between Au^{3+} ions and adenine DNA also had implications in DNAzyme activity. The addition of Au^{3+} ions at high enough concentrations inhibited the cleavage activity of the 17E DNAzyme.

4.2 Future Work

Based on this work, there are many possible directions for continuing to study the coordination of Au^{3+} and DNA. The exact structure of the coordination complex is still unknown and would benefit from being observed with methods such as x-ray crystallography. This can also give some insight on exactly where the gold is binding and what kind of conformation change it is imposing upon the DNA. The exact number of Au^{3+} that bind to each DNA is still unknown and can be studied further to find its effects on the quenching of the fluorescence.

A sensor could be developed using A_{15} for the detection of Au^{3+} ions based on fluorescence. The selectivity and sensitivity would need to be further tested using a wide range of other metals and possible substrates. The effect this interaction has on the selection process for DNAzymes and aptamers can also be an area of interest. Care should be taken when attempting to do selection in the presence of Au^{3+} . This study has shown that Au^{3+} will strongly bind to any adenine residue in DNA and inhibits some of its catalytic abilities.

Only one DNAzyme (17E) was studied for the effects of Au^{3+} . More studies can be done with a greater variety of DNAzymes to observe the inhibitory or other effects. This can then be expanded to other DNA aptamers and DNA in general.

Chapter 5 - Lab Safety

General lab safety should be observed at all times. This includes the wearing of personal protective equipment such as goggles, gloves, and lab coats. Safety data sheets should also be referred to routinely and be kept in an accessible area. Samples and preparations should be used inside a fume hood including weighing of powders and other volatile substances. Flammable solvents should be kept in separate areas specific to flammables. All waste must be sorted and disposed of accordingly. Appropriate safety training such as the Workplace Hazardous Materials Information System (WHMIS) 2015 must be completed prior to entry in the lab. The locations of the emergency supplies and equipment such as eyewash stations, spill kits, fire extinguishers, and emergency showers should be known and easily accessed. Ultraviolet light is also known to damage the eyes and special glasses should be worn. While working with these chemicals and procedures, the appropriate personal protective equipment must always be worn. In order to use the gel electrophoresis apparatus, precautions must be taken to avoid electric shock. Before connecting or disconnecting leads, hands must be dry and gloved. The apparatus should be kept away from sinks and other sources of water. Heavy metal salts must also be handled with caution as gold salts can cause irritation or corrosion of the skin as well as cause serious eye damage.

References

1. Zhou, W., Saran, R. & Liu, J. Metal Sensing by DNA. *Chem. Rev.* **117**, 8272–8325 (2017).
2. Li, J. & Lu, Y. A highly sensitive and selective catalytic DNA biosensor for lead ions. *J. Am. Chem. Soc.* **122**, 10466–10467 (2000).
3. Hartwig, J. F. & Lippard, S. J. DNA Binding Properties of cis-[Pt(NH₃)(C₆H₁₁NH₂)Cl₂], a Metabolite of an Orally Active Platinum Anticancer Drug. *J. Am. Chem. Soc.* **114**, 5646–5654 (1992).
4. Zhang, X.-B., Kong, R.-M. & Lu, Y. Metal Ion Sensors Based on DNAzymes and Related DNA Molecules. *Annu. Rev. Anal. Chem.* **4**, 105–128 (2011).
5. Izatt, R. M., Christensen, J. J. & Rytting, J. H. Sites and Thermodynamic Quantities Associated With Proton and Metal Ion Interaction With Ribonucleic Acid. *Chem. Rev.* **501**, 439–481 (1971).
6. Dingley, A. J., Masse, J. E., Peterson, R. D., Barfield, M., Feigon, J. & Grzesiek, S. Internucleotide scalar couplings across hydrogen bonds in Watson-Crick and Hoogsteen base pairs of a DNA triplex. *J. Am. Chem. Soc.* **121**, 6019–6027 (1999).
7. Sundaresan, N. & Suresh, C. H. A base-sugar-phosphate three-layer ONIOM model for cation binding: Relative binding affinities of alkali metal ions for phosphate anion in DNA. *J. Chem. Theory Comput.* **3**, 1172–1182 (2007).
8. Sigel, R. K. O. & Sigel, H. A stability concept for metal ion coordination to single-stranded nucleic acids and affinities of individual sites. *Acc. Chem. Res.* **43**, 974–984 (2010).
9. Izatt, R. M., Christensen, J. J. & Rytting, J. H. Sites and thermodynamic quantities associated with proton and metal ion interaction with ribonucleic acid, deoxyribonucleic acid, and their constituent bases, nucleosides, and nucleotides. *Chem. Rev.* **71**, 439–481 (1971).
10. Lippert, B. Chapter 2 Coordinative Bond Formation Between Metal Ions and Nucleic Acid Bases. in *Nucleic Acid-Metal Ion Interactions* 39–74 (The Royal Society of Chemistry, 2009). doi:10.1039/9781847558763-00039
11. Pillai, C. K. S. & Nandi, U. S. Binding of gold(III) with DNA. *Biopolymers* **12**, 1431–1435 (1973).
12. Pu, F., Ren, J. & Qu, X. Nucleobases, nucleosides, and nucleotides: versatile biomolecules for generating functional nanomaterials. *Chem. Soc. Rev.* **47**, 1285–1306 (2018).
13. Lippert, B. & Sanz Miguel, P. J. The Renaissance of Metal-Pyrimidine Nucleobase Coordination Chemistry. *Acc. Chem. Res.* **49**, 1537–1545 (2016).
14. Kazakov, S. A. & Hecht, S. M. *Nucleic Acid-Metal Ion Interactions*. *Encyclopedia of Inorganic Chemistry* (2006). doi:10.1002/0470862106.ia166
15. Lippert, B. Multiplicity of metal ion binding patterns to nucleobases. *Coord. Chem. Rev.* **200–202**, 487–516 (2000).
16. Šponer, J., Šponer, J. E., Gorb, L., Leszczynski, J. & Lippert, B. Metal-stabilized rare tautomers and mispairs of DNA bases: N₆-metalated adenine and N₄-metalated cytosine, theoretical and experimental views. *J. Phys. Chem. A* **103**, 11406–11413 (1999).
17. Zamora, F., Kunsman, M., Sabat, M. & Lippert, B. Metal-Stabilized Rare Tautomers of

- Nucleobases. 6. Imino Tautomer of Adenine in a Mixed-Nucleobase Complex of Mercury(II). *Inorg. Chem.* **36**, 1583–1587 (1997).
18. Lippert, B., Schollhorn, H. & Thewalt, U. Metal-Stabilized Rare Tautomers of Nucleobases. 1. Imino-oxo Form of Cytosine: Formation through Metal Migration and Estimation of the Geometry of the Free Tautomer. *J. Am. Chem. Soc.* **108**, 6616–6621 (1986).
 19. Liang, H., Lin, F., Zhang, Z., Liu, B., Jiang, S., Yuan, Q. & Liu, J. Multicopper laccase mimicking nanozymes with nucleotides as ligands. *ACS Appl. Mater. Interfaces* **9**, 1352–1360 (2017).
 20. Ono, A., Torigoe, H., Tanaka, Y. & Okamoto, I. Binding of metal ions by pyrimidine base pairs in DNA duplexes. *Chem. Soc. Rev* **40**, 5855–5866 (2011).
 21. Liu, X., Atwater, M., Wang, J. & Huo, Q. Extinction coefficient of gold nanoparticles with different sizes and different capping ligands. *Colloids Surfaces B Biointerfaces* **58**, 3–7 (2007).
 22. Rosi, N. L. & Mirkin, C. A. Nanostructures in biodiagnostics. *Chemical Reviews* **105**, 1547–1562 (2005).
 23. Dubertret, B., Calame, M. & Libchaber, A. J. Single-mismatch detection using gold-quenched fluorescent oligonucleotides. *Nat. Biotechnol.* **19**, 365–370 (2001).
 24. Smith, T. *The Hydrophilic Nature of a Clean Gold Surface*. (1980).
 25. Frens, G. Controlled Nucleation for the Regulation of the Particle Size in Monodisperse Gold Suspensions. *Nat. Phys. Sci.* **241**, 20–22 (1973).
 26. Pamies, R., Cifre, J. G. H., Espín, V. F., Collado-González, M., Baños, F. G. D. & De La Torre, J. G. Aggregation behaviour of gold nanoparticles in saline aqueous media. *J. Nanoparticle Res.* **16**, (2014).
 27. Xi, W. & Haes, A. J. Elucidation of HEPES Affinity to and Structure on Gold Nanostars. *J. Am. Chem. Soc.* **141**, 4034–4042 (2019).
 28. Zhang, X., Servos, M. R. & Liu, J. Surface science of DNA adsorption onto citrate-capped gold nanoparticles. *Langmuir* **28**, 3896–3902 (2012).
 29. Kimura-Suda, H., Petrovykh, D. Y., Tarlov, M. J. & Whitman, L. J. Base-dependent competitive adsorption of single-stranded DNA on gold. *J. Am. Chem. Soc.* **125**, 9014–9015 (2003).
 30. Shiddiky, M. J. A., Koo, K. M., Trau, M., Carrascosa, L. G. & Sina, A. A. I. DNA–bare gold affinity interactions: mechanism and applications in biosensing. *Anal. Methods* **7**, 7042–7054 (2015).
 31. Jang, N.-H. The Coordination Chemistry of DNA Nucleosides on Gold Nanoparticles as a Probe by SERS. *Bull. Korean Chem. Soc.* **23**, 1790–1800 (2002).
 32. Pergolese, B., Bonifacio, A. & Bigotto, A. SERS studies of the adsorption of guanine derivatives on gold colloidal nanoparticles. *Phys. Chem. Chem. Phys.* **7**, 3610–3613 (2005).
 33. Piana, S. & Bilic, A. The nature of the adsorption of nucleobases on the gold [111] surface. *J. Phys. Chem. B* **110**, 23467–23471 (2006).
 34. Östblom, M., Liedberg, B., Demers, L. M. & Mirkin, C. A. On the structure and desorption dynamics of DNA bases adsorbed on gold: A temperature-programmed study. *J. Phys. Chem. B* **109**, 15150–15160 (2005).

35. Sandström, P., Boncheva, M. & Åkerman, B. Nonspecific and thiol-specific binding of DNA to gold nanoparticles. *Langmuir* **19**, 7537–7543 (2003).
36. Cárdenas, M., Barauskas, J., Schullén, K., Brennan, J. L., Brust, M. & Nylander, T. Thiol-specific and nonspecific interactions between DNA and gold nanoparticles. *Langmuir* **22**, 3294–3299 (2006).
37. Zhou, W., Wang, F., Ding, J. & Liu, J. Tandem phosphorothioate modifications for DNA adsorption strength and polarity control on gold nanoparticles. *ACS Appl. Mater. Interfaces* **6**, 14795–14800 (2014).
38. Inkpen, M. S., Liu, Z., Li, H., Campos, L. M., Neaton, J. B. & Venkataraman, L. Non-chemisorbed gold–sulfur binding prevails in self-assembled monolayers. *Nat. Chem.* **11**, 351–358 (2019).
39. Liu, B., Kelly, E. Y. & Liu, J. Cation-size-dependent DNA adsorption kinetics and packing density on gold nanoparticles: An opposite trend. *Langmuir* **30**, 13228–13234 (2014).
40. Liu, B., Wu, P., Huang, Z., Ma, L. & Liu, J. Bromide as a Robust Backfiller on Gold for Precise Control of DNA Conformation and High Stability of Spherical Nucleic Acids. *J. Am. Chem. Soc.* **140**, 4499–4502 (2018).
41. Zong, C., Zhang, Z., Liu, B. & Liu, J. Adsorption of Arsenite on Gold Nanoparticles Studied with DNA Oligonucleotide Probes. *Langmuir* **35**, 7304–7311 (2019).
42. Hurst, S. J., Lytton-Jean, A. K. R. & Mirkin, C. A. Maximizing DNA loading on a range of gold nanoparticle sizes. *Anal. Chem.* **78**, 8313–8318 (2006).
43. Krishnamurthy, R. Role of pKa of nucleobases in the origins of chemical evolution. *Acc. Chem. Res.* **45**, 2035–2044 (2012).
44. Zhang, X., Servos, M. R. & Liu, J. Instantaneous and quantitative functionalization of gold nanoparticles with thiolated DNA using a pH-assisted and surfactant-free route. *J. Am. Chem. Soc.* **134**, 7266–7269 (2012).
45. Huang, Z., Liu, B. & Liu, J. Parallel Polyadenine Duplex Formation at Low pH Facilitates DNA Conjugation onto Gold Nanoparticles. *Langmuir* **32**, 11986–11992 (2016).
46. Chakraborty, S., Sharma, S., Maiti, P. K. & Krishnan, Y. The poly dA helix: a new structural motif for high performance DNA-based molecular switches. *Nucleic Acids Res.* **37**, 2810–2817 (2009).
47. Liu, B. & Liu, J. Freezing Directed Construction of Bio/Nano Interfaces: Reagentless Conjugation, Denser Spherical Nucleic Acids, and Better Nanoflakes. *J. Am. Chem. Soc.* **139**, 9471–9474 (2017).
48. Liu, B., Wu, T., Huang, Z., Liu, Y. & Liu, J. Freezing-directed Stretching and Alignment of DNA Oligonucleotides. *Angew. Chemie* **131**, 2131–2135 (2019).
49. Liu, B. & Liu, J. Freezing-Driven DNA Adsorption on Gold Nanoparticles: Tolerating Extremely Low Salt Concentration but Requiring High DNA Concentration. *Langmuir* **35**, 6476–6482 (2019).
50. Pei, H., Li, F., Wan, Y., Wei, M., Liu, H., Su, Y., Chen, N., Huang, Q. & Fan, C. Designed diblock oligonucleotide for the synthesis of spatially isolated and highly hybridizable functionalization of DNA-gold nanoparticle nanoconjugates. *J. Am. Chem. Soc.* **134**, 11876–11879

- (2012).
51. Lin, M., Wang, J., Zhou, G., Wang, J., Wu, N., Lu, J., Gao, J., Chen, X., Shi, J., Zuo, X. & Fan, C. Programmable engineering of a biosensing interface with tetrahedral DNA nanostructures for ultrasensitive DNA detection. *Angew. Chemie - Int. Ed.* **54**, 2151–2155 (2015).
 52. Reynolds, R. A., Mirkin, C. A. & Letsinger, R. L. Homogeneous, nanoparticle-based quantitative colorimetric detection of oligonucleotides [13]. *Journal of the American Chemical Society* **122**, 3795–3796 (2000).
 53. Elghanian, R., Storhoff, J. J., Mucic, R. C., Letsinger, R. L. & Mirkin, C. A. Selective colorimetric detection of polynucleotides based on the distance-dependent optical properties of gold nanoparticles. *Science (80-.)*. **277**, 1078–1081 (1997).
 54. Ray, P. C., Fortner, A. & Darbha, G. K. Gold Nanoparticle Based FRET Assay for the Detection of DNA Cleavage. *J. Phys. Chem. B* **110**, 20745–20748 (2006).
 55. Seferos, D. S., Giljohann, D. A., Hill, H. D., Prigodich, A. E. & Mirkin, C. A. Nano-flares: Probes for transfection and mRNA detection in living cells. *J. Am. Chem. Soc.* **129**, 15477–15479 (2007).
 56. Pillai, C. K. S. & Nandi, U. S. Interaction of metal ions with nucleic acids and related compounds. II. Studies on Au(III)-nucleic acid system. *Biopolymers* **17**, 709–729 (1978).
 57. Ennifar, E., Walter, P. & Dumas, P. A crystallographic study of the binding of 13 metal ions of two related RNA duplexes. *Nucleic Acids Res.* **31**, 2671–2682 (2003).
 58. Lippert, B. Metal-Nucleobase Chemistry: Coordination, Reactivity, and Base Pairing. in *Bioinorganic Chemistry* 179–199 (Springer Netherlands, 1995). doi:10.1007/978-94-011-0255-1_15
 59. Du, J., Wang, Z., Fan, J. & Peng, X. Gold nanoparticle-based colorimetric detection of mercury ion via coordination chemistry. *Sensors Actuators B* **212**, 481–486 (2015).
 60. Bressan, M., Ettore, R. & Rigo, P. NMR Studies of the Interaction between Cytosine and Gold Complexes. *J. Magn. Reson.* **26**, 43–84 (1977).
 61. Holowczak, M. S., Stancl, M. D. & Wong, G. B. Trichloro(1-methylcytosinato)gold(III). Model for Gold-DNA Interactions. *J. Am. Chem. Soc.* **107**, 5789–5790 (1985).
 62. Wu, Z. S., Guo, M. M., Shen, G. L. & Yu, R. Q. G-rich oligonucleotide-functionalized gold nanoparticle aggregation. *Anal. Bioanal. Chem.* **387**, 2623–2626 (2007).
 63. Schimanski, A., Freisinger, E., Erxleben, A. & Lippert, B. Interactions between [AuX₄]⁻ (X = Cl, CN) and cytosine and guanine model nucleobases: Salt formation with (hemi-) protonated bases, coordination, and oxidative degradation of guanine. *Inorganica Chim. Acta* **283**, 223–232 (1998).
 64. Wei, H., Li, B., Du, Y., Dong, S. & Wang, E. Nucleobase-metal hybrid materials: Preparation of submicrometer-scale, spherical colloidal particles of adenine-gold(III) via a supramolecular hierarchical self-assembly approach. *Chem. Mater.* **19**, 2987–2993 (2007).
 65. Lopez, A. & Liu, J. Light-activated metal-coordinated supramolecular complexes with charge-directed self-assembly. *J. Phys. Chem. C* **117**, 3653–3661 (2013).
 66. Wang, F., Liu, B., Huang, P.-J. J. & Liu, J. Rationally Designed Nucleobase and Nucleotide Coordinated Nanoparticles for Selective DNA Adsorption and Detection. *Anal. Chem.* **85**, 16 (2013).

67. Gibson, D. W., Beer, M. & Barnett, R. J. Gold (111) Complexes of Adenine Nucleotides*. *Biochemistry* **10**, 3669–3679 (1971).
68. Wu, Y. & Lai, R. Y. Electrochemical Gold(III) Sensor with High Sensitivity and Tunable Dynamic Range. *Anal. Chem* **88**, 2227–2233 (2016).
69. Christianson, A. M. & Gabbai, F. P. Synthesis and Coordination Chemistry of a Phosphine-Decorated Fluorescein: ‘double Turn-On’ Sensing of Gold(III) Ions in Water. *Inorg. Chem.* **55**, 5828–5835 (2016).
70. Megarajan, S., Kamlekar, R. K., Kumar, P. S. & Anbazhagan, V. Rapid and selective colorimetric sensing of Au³⁺ ions based on galvanic displacement of silver nanoparticles. *New J. Chem.* **43**, 18741–18746 (2019).
71. Yang, B., Zhang, X. B., Liu, W. N., Hu, R., Tan, W., Shen, G. L. & Yu, R. Q. Fluorosurfactant-capped gold nanoparticles-based label-free colorimetric assay for Au³⁺ with tunable dynamic range via a redox strategy. *Biosens. Bioelectron.* **48**, 1–5 (2013).
72. Egorova, O. A., Seo, H., Chatterjee, A. & Ahn, K. H. Reaction-based fluorescent sensing of Au(I)/Au(III) species: Mechanistic implications on vinylgold intermediates. *Org. Lett.* **12**, 401–403 (2010).
73. Do, J. H., Kim, H. N., Yoon, J., Kim, J. S. & Kim, H. J. A rationally designed fluorescence turn-on probe for the gold(III) ion. *Org. Lett.* **12**, 932–934 (2010).
74. Breaker, R. R. & Joyce, G. F. A DNA enzyme that cleaves RNA. *Chem. Biol.* **1**, 223–229 (1994).
75. Pulimamidi Rabindra Reddy and Nomula Raju (April 4th 2012). Gel-Electrophoresis and Its Applications, Gel Electrophoresis - Principles and Basics, Sameh Magdeldin, IntechOpen, DOI: 10.5772/38479. Available from: <https://www.intechopen.com/books/gel-electrophoresis-principles-and-basics/gel-electrophoresis-and-its-applications>
76. National Diagnostics. Denaturing Polyacrylamide Gel Electrophoresis of DNA and RNA. (2011). Available at: <https://www.nationaldiagnostics.com/electrophoresis/article/denaturing-polyacrylamide-gel-electrophoresis-dna-rna>. (Accessed: 26th February 2019)
77. Wuithschick, M., Birnbaum, A., Witte, S., Sztucki, M., Vainio, U., Pinna, N., Rademann, K., Emmerling, F., Kraehnert, R. & Rg Polte, J. Turkevich in New Robes :Key Questions Answered for the Most Common Gold Nanoparticle Synthesis. *ACS Nano* **9**, 7052–7071 (2015).
78. Huang, P.-J. J., Jabari, A., Fong, L. L. C., Saran, R. & Liu, J. *Modulation of Au³⁺ Assisted Cleavage of Phosphorothioate-Modified DNAzyme by Halides.* (2020).
79. Ellington, A. D. & Szostak, J. W. In vitro selection of RNA molecules that bind specific ligands. *Nature* **346**, 818–822 (1990).
80. Ellington, A. D. & Szostak, J. W. Selection in vitro of single-stranded DNA molecules that fold into specific ligand-binding structures. *Nature* **355**, 850–852 (1992).
81. Fan, C., Wang, L., Song, S., Zhao, J. & Li, J. Aptamer-based biosensors. *TrAC Trends Anal. Chem.* **27**, 108–117 (2007).
82. Shahdordizadeh, M., Taghdisi, S. M., Ansari, N., Alebooye Langroodi, F., Abnous, K. & Ramezani, M. Aptamer based biosensors for detection of Staphylococcus aureus. *Sensors Actuators, B Chem.* **241**, 619–635 (2017).
83. Basu, S., Jana, S., Pande, S. & Pal, T. Interaction of DNA bases with silver nanoparticles:

- Assembly quantified through SPRS and SERS. *J. Colloid Interface Sci.* **321**, 288–293 (2008).
84. Zhao, W., Chiuman, W., Lam, J. C. F., Mcmanus, S. A., Chen, W., Cui, Y., Pelton, R., Brook, M. A. & Li, Y. DNA Aptamer Folding on Gold Nanoparticles: From Colloid Chemistry to Biosensors. *J. Am. Chem. Soc.* **130**, 3610–3618 (2008).
 85. Lu, Y. New transition-metal-dependent DNAzymes as efficient endonucleases and as selective metal biosensors. *Chem. - A Eur. J.* **8**, 4588–4596 (2002).
 86. Kim, H.-K., Rasnik, I., Liu, J., Ha, T. & Lu, Y. Dissecting metal ion-dependent folding and catalysis of a single DNAzyme. *Nat. Chem. Biol.* **3**, 763–768 (2007).
 87. Hollenstein, M. DNA Catalysis: The Chemical Repertoire of DNAzymes. *Molecules* **20**, 20777–20804 (2015).
 88. Hollenstein, M., Hipolito, C., Lam, C., Dietrich, D. & Perrin, D. M. A Highly Selective DNAzyme Sensor for Mercuric Ions. *Angew. Chemie* **120**, 4418–4422 (2008).
 89. Lan, T., Furuya, K. & Lu, Y. A highly selective lead sensor based on a classic lead DNAzyme. *Chem. Commun.* **46**, 3896–3898 (2010).
 90. Chen, Y., Li, H., Gao, T., Zhang, T., Xu, L., Wang, B., Wang, J. & Pei, R. Selection of DNA aptamers for the development of light-up biosensor to detect Pb(II). *Sensors Actuators, B Chem.* **254**, 214–221 (2018).
 91. Xue, X., Wang, F. & Liu, X. One-step, room temperature, colorimetric detection of mercury (Hg²⁺) using DNA/nanoparticle conjugates. *J. Am. Chem. Soc.* **130**, 3244–3245 (2008).
 92. Li, J. In vitro selection and characterization of a highly efficient Zn(II)-dependent RNA-cleaving deoxyribozyme. *Nucleic Acids Res.* **28**, 481–488 (2000).